university of groningen

faculty of science and engineering

AMOC transitions: spurious or fragmented tipping?

Aldo Zanuttini

university of groningen / faculty of science and engineering

University of Groningen

AMOC transitions: spurious or fragmented tipping?

Master's Thesis

To fulfill the requirements for the degree of
Master of Science in Mathematics
at University of Groningen under the supervision of
dr. F.W. Wubs (Bernoulli Institute, University of Groningen)
Prof. dr. H.A. Dijkstra (Institute for Marine and Atmospheric Research, Utrecht),
and
dr. J. Koellermeier (Bernoulli Institute, University of Groningen)

Aldo Zanuttini (s3451062)

July 9, 2024

Abstract

This thesis investigates the claim that the multiple equilibria found in large scale ocean models are spurious. The investigation is carried out using finite volume discretizations, and numerical bifurcation analysis on two modified ocean convection models. Phenomena responsible for coexistence states and pattern formation will be of particular interest, such as fragmented tipping and the theory of Turing instabilities. The main results are that at least some of the multiple equilibria in the large scale model are likely due to fragmented tipping, and that a localized Turing bifurcation occurs one of the conceptual models.

Contents

1 Introduction **2**

2 Numerical methods **2**
2.1 Finite Volume method . . . 2
2.2 Modified Moore-Penrose continuation . . . 3

3 Modified den Toom model **5**
3.1 The model . . . 5
3.2 Discretization . . . 6
3.2.1 Without Convective Adjustment . . . 6
3.2.2 Finite Volume discretization of the Convective Adjustment . . . 8
3.3 Linearization . . . 9
3.4 Eigenvalue Analysis . . . 11
3.4.1 Decoupled case . . . 11
3.4.2 Coupled case . . . 12
3.5 Numerical Results . . . 13
3.5.1 Analytical Verification of Numerical Results . . . 13
3.5.2 Numerical Results when using $\mathcal{F}_1$ . . . 16
3.5.3 Numerical Results when using $\mathcal{F}_2$ . . . 18
3.5.4 Discussion . . . 20

4 Modified Bastiaansen model **20**
4.1 Discretization . . . 22
4.1.1 Without Convective Adjustment . . . 22
4.1.2 Discretization of the Convective Adjustment . . . 24
4.2 Linearization and Eigenvalue Analysis . . . 25
4.3 Numerical Results . . . 27
4.4 Discussion . . . 29

5 Spuriousness of the multiple equilibria in the original den Toom models **30**
5.1 Spatial Dynamics of the den Toom model . . . 30
5.1.1 Decoupled case . . . 31
5.1.2 Coupled case . . . 32
5.2 Localized Turing Instability . . . 33

6 Conclusion 35

1 Introduction

There has been a lot of debate recently within the field of oceanography and more broadly climate science, over the effect that increased freshwater forcing will have on the Atlantic Meriodional Overturning Circulation (AMOC). The question is whether there is multi-stability or bistability. In more mathematical language: how many (stable) equilibria the system has. Recent results [11] would in fact suggest that (depending on the freshwater forcing) there can be up to 9 stable equilibria, which correspond to scenarios where the AMOC weakens in some parts of the spatial domain and not in others. Skeptics on the other hand, claim these multiple equilibria are in fact spurious [15].

In this thesis we will study two dimensional generalizations of two conceptual models for the AMOC: one which we will refer to as the *modified den Toom model* [15], and the other which we shall refer to as the *modified Bastiaansen model* [1]. The former, in its one dimensional formulation, has been suggested (not proven) to have spurious multiple equilibria, while the other exhibits *fragmented tipping* when studied in one spatial dimension. While there is no formal mathematical definition of what fragmented tipping is, roughly speaking this refers to the appearance of new fold bifurcations in the vicinity of existing ones, due to the inclusion of diffusion and spatial heterogeneity in an otherwise finite dimensional dynamical system. This phenomenon is caused by the appearance of *coexistence states*, that is steady states where the domain lies in multiple states at once. Intuitively one can think of equilibrium planetary ice-cover as solar radiation is varied: in absence of diffusion a planet can be either entirely ice free or entirely covered in ice, while when one adds diffusion it is also possible that part of the celestial body is covered in ice and the remainder is ice free.

We will begin with the study of the two dimensional den Toom model, presented in section 2, which we will discretize and then study, first analytically and then numerically. We will then repeat the same process for the Bastiaansen model, finding a very similar bifurcation pattern. Finally we will turn to spatial dynamics and Turing bifurcations to attempt to explain our numerical findings.

2 Numerical methods

In this section we will discuss the discretization and continuation methods used throughout this thesis.

2.1 Finite Volume method

Throughout this thesis we will discretize systems of PDE using the finite volume method [4]. Suppose the PDE to be discretized has the form

$$u_t = \mathcal{L}u - f, \quad \mathcal{L} = \nabla \cdot (\mathcal{M}u)$$

where $\mathcal{M}$ is some operator which transforms a scalar function into a two or three-dimensional vector function. Integrating both sides we have that

$$\frac{d}{dt}\int_\Omega u d\Omega = \int_\Omega \nabla \cdot (\mathcal{M}u) - f d\Omega.$$

Application of the Guass theorem yields

$$\frac{d}{dt}\int_\Omega u d\Omega = \int_\Gamma (\mathcal{M}u, \vec{n}) d\Gamma - \int_\Omega f d\Omega$$

where $\Gamma = \partial\Omega$ denotes the boundary of the domain. Note that if

$$\int_\Gamma (\mathcal{M}u, \vec{n}) d\Gamma - \int_\Omega f d\Omega = 0$$

then $\int_\Omega u d\Omega$ is conserved.

Next we cover the domain Ω by a number of *volumes* Ω_i so that

$$\frac{d}{dt}\int_{\Omega_i} u d\Omega = \int_{\Gamma_i} (\widehat{\mathcal{M}u}, \vec{n}) d\Gamma - \int_{\Omega_i} f d\Omega$$

where $\Gamma_i = \sum_{j\in\mathcal{N}(i)} \Gamma_{ij}$ and $\mathcal{N}(i)$ contains the indices of volumes neighbouring volume i. It can be shown that using this method, if $\int_\Omega u d\Omega$ is conserved in the continuous case, then it must also be conserved in the discrete case.

2.2 Modified Moore-Penrose continuation

Throughout this thesis we will be showing multiple bifurcation diagrams. These are computed using a modified version of the *Moore-Penrose* continuation method [10]. This is a predictor-corrector method, this means that the method consists of two steps: (tangent) prediction and correction.

Consider a dynamical system of the form

$$\dot{x} = f(x, \alpha), \quad x \in \mathbb{R}^n, \quad \alpha \in \mathbb{R}$$

an equilibrium of this system is a value $x^*(\alpha)$ such that $f(x^*(\alpha), \alpha) = 0$. This defines a (typically) smooth one-dimensional manifold $M \subset \mathbb{R}^{n+1}$. Letting $y = (x, \alpha)$ and defining $F(y) = f(x, \alpha)$, the *continuation problem* is then to find y such that

$$F(y) = 0, \quad F : \mathbb{R}^{n+1} \longrightarrow \mathbb{R}.$$

Using the Implicit Function Theorem, we know the above locally defines a smooth curve M passing through a point y_0 so long as the regularity condition:

$$\text{rank}(J(y_0)) = n, \quad J = F_y(y) \in \mathbb{R}^{n\times(n+1)}.$$

To approximate the curve M we need to find a sequence of points $(y_0, y_1, \ldots y_n)$ satisfying $F(y_i) = 0$. Note that y_0 is often a known value, however there are continuation problems where this might need to be computed using some kind of root-finding algorithm (as we

shall do in most of this thesis). Suppose the point y_i is known, then we can predict where the next point y_{i+1} on M will be located by making a prediction $\overline{y}_i$ as

$$\overline{y}_i = y_i + s_i v_i$$

where $s_i \in \mathbb{R}$ is called the *step size* which in principle can be chosen arbitrarily (however there are better and worse ways of choosing it), while v_i is the (normalized) nontrivial solution to

$$J(y_i)v_i = 0, \quad ||v_i|| = 1$$

(equivalently: v_i is the tangent to M at the point y_i). When performing continuation, it is convenient to proceed in the same direction along M. A good way to ensure that $\langle v_{i-1}, v_i \rangle = 1$ (that is: the direction is preserved) is to compute v_i as

$$\begin{bmatrix} J \\ v_{i-1}^T \end{bmatrix} v_i = \begin{bmatrix} 0 \\ 1 \end{bmatrix}.$$

For the correction step, let $X_0 = \overline{y}_i$, then define

$$X_{n+1} = X_n - F_x(X_n)^+ F(X_n)$$

where $F_x(X_i)^+$ denotes the Moore-Penrose Pseudoinverse of $F_x(X_i)$. Finally let $V_0 = v_i$ and define V_n to be the solution to

$$\begin{bmatrix} J \\ V_{n-1}^T \end{bmatrix} V_n = \begin{bmatrix} 0 \\ 1 \end{bmatrix}.$$

Then as soon as the conditions

$$||X_n - X_{n-1}|| < \varepsilon_1, \quad ||F(X_n)|| < \varepsilon_2, \quad v_i^T V_n > 0$$

are all verified, we set $y_{i+1} = X_n$ and repeat the prediction step.

All of the above describes in detail the functioning of the Moore-Penrose continuation scheme, the only difference with this scheme that we implemented is in the Newton iterations that define X_{n+1}. For this we instead resort to a sixth order method [16], which looks like this

$$\begin{aligned} Y_n &= X_n - F_x(X_n)^+ F(X_n) \\ Z_n &= Y_n - (2I - F_x(X_n)^+ F_x(Y_n)) F_x(X_n)^+ F(Y_n) \\ X_{n+1} &= Z_n - (2I - F_x(X_n)^+ F_x(Y_n)) F_x(X_n)^+ F(Z_n). \end{aligned}$$

The method is sixth-order in the sense that, letting α be the true solution to $F(x) = 0$ (i.e. $F(\alpha) = 0$) and $e_n = X_n - \alpha$ be the true error at step n, then [16]

$$e_{n+1} = (\frac{1}{2} F_x(\alpha)^{-1} F_{xx}(\alpha))^5 30 e_n^6 + \mathcal{O}(e^7).$$

This may not look like much as at each computation of X_n three Newton-like iterations must be carried out, but when compared to three ordinary Newton iterations, this method reduces the number of evaluations of the Jacobian by 1. There are other (perhaps computationally simpler) methods to obtain a more accurate Moore-Penrose scheme, however these often rely on higher order derivatives to be implemented, making computations by hand far more complicated and requiring efficient solvers for nonlinear vector equations.

3 Modified den Toom model

3.1 The model

In the first part of this project, we study a modified version of the model studied in [15]. The modified system is given by:

$$\frac{\partial T_*}{\partial t_*} = K_V \frac{\partial}{\partial z_*}([1 + C_T(T_*, S_*)]\frac{\partial T_*}{\partial z_*}) - \kappa(i_T^{res} T_* - \overline{T}_*(x_*, z_*)) + K_H \frac{\partial^2 T_*}{\partial x_*^2}$$
$$\frac{\partial S_*}{\partial t_*} = K_V \frac{\partial}{\partial z_*}([1 + C_S(T_*, S_*)]\frac{\partial S_*}{\partial z_*}) - \kappa(i_S^{res} S_* - \overline{S}_*(x_*, z_*)) + K_H \frac{\partial^2 S_*}{\partial x_*^2}$$

with zero-flux boundary conditions across all boundaries ($x = 0, L$ and $z = 0, D$).

By making the substitutions:

$$t = \kappa t_*, \quad z = D^{-1} z_*, \quad x = L^{-1} x_*,$$
$$T = \alpha_T(T_* - T_0), \quad S = \alpha_S(S_* - S_0)$$

the system can be nondimensionalized, giving:

$$\frac{\partial T}{\partial t} = \frac{1}{P_v}\frac{\partial}{\partial z}([1 + C_T(T, S)]\frac{\partial T}{\partial z}) - (i_T^{res} T - \overline{T}(x, z)) + \frac{1}{P_h}\frac{\partial^2 T}{\partial x^2}$$
$$\frac{\partial S}{\partial t} = \frac{1}{P_v}\frac{\partial}{\partial z}([1 + C_S(T, S)]\frac{\partial S}{\partial z}) - (i_S^{res} S - \overline{S}(x, z)) + \frac{1}{P_h}\frac{\partial^2 S}{\partial x^2}.$$

Finally, defining $\rho = S - T$ (the density) and $\mu = S + T$ (the spiciness), one obtains:

$$\frac{\partial \rho}{\partial t} = \frac{1}{P_v}\frac{\partial}{\partial z}((1 + C(\frac{\partial \rho}{\partial z}))\frac{\partial \rho}{\partial z}) - (i_+^{res}\rho + i_-^{res}\mu - \bar{\rho}(x, z; \gamma)) + \frac{1}{P_h}\frac{\partial^2 \rho}{\partial x^2} \tag{1a}$$
$$\frac{\partial \mu}{\partial t} = \frac{1}{P_v}\frac{\partial}{\partial z}((1 + C(\frac{\partial \rho}{\partial z}))\frac{\partial \mu}{\partial z}) - (i_-^{res}\rho + i_+^{res}\mu - \bar{\mu}(x, z; \gamma)) + \frac{1}{P_h}\frac{\partial^2 \mu}{\partial x^2} \tag{1b}$$

where $P_v = \frac{D^2\kappa}{K_V}$, $P_h = \frac{L^2\kappa}{K_H}$ can be interpreted to be the vertical and horizontal Péclet numbers and

$$C(\frac{\partial \rho}{\partial z}) = F_0 \mathcal{G}(\frac{\partial \rho}{\partial z})$$

where we will treat separately the cases:

$$\mathcal{G}(\frac{\partial \rho}{\partial z}) = \frac{1}{2}(1 + \tanh(\varepsilon\frac{\partial \rho}{\partial z})) =: \mathcal{F}_1(\frac{\partial \rho}{\partial z})$$
$$\mathcal{G}(\frac{\partial \rho}{\partial z}) = \max(0, \tanh^3(\varepsilon\frac{\partial \rho}{\partial z})) =: \mathcal{F}_2(\frac{\partial \rho}{\partial z}).$$

Further we have:

$$\overline{\rho} = \overline{S} - \overline{T} = \delta(x)(\gamma\cos(\pi z) - \cos(2\pi z))$$
$$\overline{\mu} = \overline{S} + \overline{T} = \delta(x)(\gamma\cos(\pi z) + \cos(2\pi z))$$

an we choose $\delta(x) = \cos(\frac{\pi x}{2})$.

Finally also note that the steady state of system (1) is underdetermined when

$$i_+^{res} + i_-^{res} = i_S^{res} = 0, \quad \text{or} \quad i_+^{res} - i_-^{res} = i_T^{res} = 0$$

so whenever we make such a choice for these parameters we must also augment the system with the integral constraints

$$\int_\Omega T d\Omega = 0, \quad \text{if} \quad i_+^{res} - i_-^{res} = 0$$
$$\int_\Omega S d\Omega = 0, \quad \text{if} \quad i_+^{res} + i_-^{res} = 0.$$

These constraints are not needed when solving for the transient case, as the initial conditions specifies the levels of ρ and μ.

3.2 Discretization

3.2.1 Without Convective Adjustment

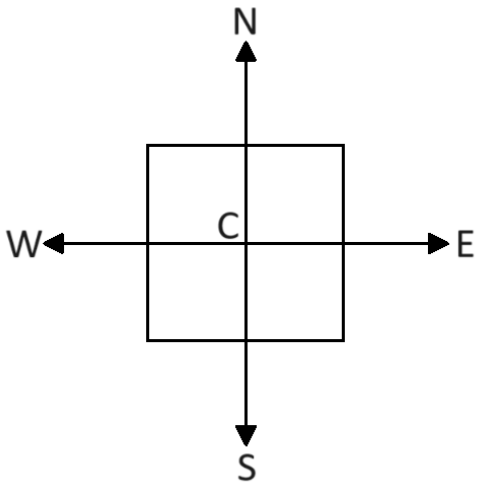

Figure 1: An example of the type of conservation cell used in the discretization, neighboring cell centers are labelled N, E, W, S. The center of the cell itself is labelled C.

Letting $S^\rho = -(i_+^{res}\rho + i_-^{res}\mu - \overline{\rho}(x,y;\gamma))$ and $S^\mu = -(i_-^{res}\rho + i_+^{res}\mu - \overline{\mu}(x,y;\gamma))$, the system without convective adjustment reads

$$\frac{\partial \rho}{\partial t} = \frac{1}{P_v}\frac{\partial^2 \rho}{\partial z^2} + S^\rho + \frac{1}{P_h}\frac{\partial^2 \rho}{\partial x^2}$$
$$\frac{\partial \mu}{\partial t} = \frac{1}{P_v}\frac{\partial^2 \mu}{\partial z^2} + S^\mu + \frac{1}{P_h}\frac{\partial^2 \rho}{\partial x^2}$$

by the Gauss theorem

$$\iint \frac{1}{P_v}\frac{\partial^2\rho}{\partial z^2} + S^\rho + \frac{1}{P_h}\frac{\partial^2\rho}{\partial x^2} dV = \int (\frac{1}{P_v}\frac{\partial\rho}{\partial z} + \frac{1}{P_h}\frac{\partial\rho}{\partial x}) \cdot \vec{n} dS + \iint S^\rho dV$$

covering the domain in square cells like the one in figure 1, we can discretize the above as

$$\int_{S_c} (\frac{1}{P_v}\frac{\partial\rho}{\partial z} + \frac{1}{P_h}\frac{\partial\rho}{\partial x}) \cdot \vec{n} dS + \iint_{V_c} S^\rho dV \approx$$
$$\frac{\Delta x}{P_v}(\frac{\rho_n - \rho_c}{\Delta z} - \frac{\rho_c - \rho_s}{\Delta z}) + \frac{\Delta z}{P_h}(\frac{\rho_e - \rho_c}{\Delta x} - \frac{\rho_c - \rho_w}{\Delta x}) + S_c^\rho \Delta x \Delta z$$

grouping the coefficients we obtain

$$\begin{aligned}
\rho_c: &\quad -\frac{2\Delta x}{P_v \Delta z} - \frac{2\Delta z}{P_h \Delta x} \\
\rho_n: &\quad \frac{\Delta x}{\Delta z P_v}, \qquad \rho_s: \quad \frac{\Delta x}{\Delta z P_v} \\
\rho_e: &\quad \frac{\Delta z}{\Delta x P_h}, \qquad \rho_w: \quad \frac{\Delta z}{\Delta x P_h}.
\end{aligned}$$

As for the source term, this reads

$$S_c^\rho = -i_+^{res}\rho_c + i_-^{res}\mu_c - \overline{\rho}(x_c, y_c; \gamma).$$

Along the boundaries we have

$$\begin{aligned}
\frac{\partial\rho}{\partial z} = 0 &\iff \rho_n = \rho_c = \rho_s \\
\frac{\partial\rho}{\partial x} = 0 &\iff \rho_e = \rho_c = \rho_w.
\end{aligned}$$

Thus the matrices corresponding to the x and z derivatives become

$$D_x = \begin{bmatrix}
-\frac{\Delta z}{P_h \Delta x} & \frac{\Delta z}{\Delta x P_h} & & & \\
\frac{\Delta z}{\Delta x P_h} & -\frac{2\Delta z}{\Delta x P_h} & \frac{\Delta z}{\Delta x P_h} & & \\
 & \ddots & \ddots & \ddots & \\
 & & \frac{\Delta z}{\Delta x P_h} & -\frac{2\Delta z}{\Delta x P_h} & \frac{\Delta z}{\Delta x P_h} \\
 & & & \frac{\Delta z}{\Delta x P_h} & -\frac{\Delta z}{\Delta x P_h}
\end{bmatrix} \in \mathbb{R}^{n_x \times n_x}$$

and

$$D_z = \begin{bmatrix}
-\frac{\Delta x}{P_v \Delta z} & \frac{\Delta x}{\Delta z P_v} & & & \\
\frac{\Delta x}{\Delta z P_v} & -\frac{2\Delta x}{\Delta z P_v} & \frac{\Delta x}{\Delta z P_v} & & \\
 & \ddots & \ddots & \ddots & \\
 & & \frac{\Delta x}{\Delta z P_v} & -\frac{2\Delta x}{\Delta z P_v} & \frac{\Delta x}{\Delta z P_v} \\
 & & & \frac{\Delta x}{\Delta z P_v} & -\frac{\Delta x}{\Delta z P_v}
\end{bmatrix} \in \mathbb{R}^{n_z \times n_z}$$

where n_x (resp. n_z) is the numbers of cell centers in the horizontal (resp. vertical) direction. The discretized Laplacian is then obtained via Kronecker products:

$$L = I_{nz} \otimes D_x + D_z \otimes I_{nx}.$$

The discretization of the μ equation is analogous and the discretized system reads:

$$\Delta x\Delta z\frac{d}{dt}\begin{bmatrix}\rho\\ \mu\end{bmatrix}=\begin{bmatrix}L-Ii_+^{res}\Delta x\Delta z & -Ii_-^{res}\Delta x\Delta z\\ -Ii_-^{res}\Delta x\Delta z & L-Ii_+^{res}\Delta x\Delta z\end{bmatrix}\begin{bmatrix}\rho\\ \mu\end{bmatrix}+\begin{bmatrix}\bar{\rho}\\ \bar{\mu}\end{bmatrix}\Delta x\Delta z$$

where I denotes the identity matrix. In more compact form one can write

$$M\frac{d}{dt}u=Au+M\overline{u}.$$

with $M=\Delta x\Delta z I$.

3.2.2 Finite Volume discretization of the Convective Adjustment

Note that the original system can be rewritten as

$$\begin{aligned}\frac{\partial\rho}{\partial t}&=\frac{1}{P_h}\frac{\partial^2\rho}{\partial x^2}+\frac{1}{Pv}\frac{\partial^2\rho}{\partial z^2}+S^\rho+\frac{1}{P_v}\frac{\partial}{\partial z}(C(\frac{\partial\rho}{\partial z})\frac{\partial\rho}{\partial z})\\ \frac{\partial\mu}{\partial t}&=\frac{1}{P_h}\frac{\partial^2\mu}{\partial x^2}+\frac{1}{P_v}\frac{\partial^2\mu}{\partial^2 z}+S^\mu+\frac{1}{P_v}\frac{\partial}{\partial z}(C(\frac{\partial\rho}{\partial z})\frac{\partial\mu}{\partial z})\end{aligned}$$

and that the only terms which are not included in the previous section are the rightmost ones. By the Gauss theorem we again have

$$\begin{aligned}\iint\frac{1}{P_v}\frac{\partial}{\partial z}(C(\frac{\partial\rho}{\partial z})\frac{\partial\rho}{\partial z})dV&=\frac{1}{P_v}\int(C(\frac{\partial\rho}{\partial z})\frac{\partial\rho}{\partial z})\vec{n}_z dS\\ \iint\frac{1}{P_v}\frac{\partial}{\partial z}(C(\frac{\partial\rho}{\partial z})\frac{\partial\mu}{\partial z})dV&=\frac{1}{P_v}\int(C(\frac{\partial\rho}{\partial z})\frac{\partial\mu}{\partial z})\vec{n}_z dS\end{aligned}$$

which can be discretized giving

$$\begin{aligned}\frac{1}{P_v}\int_{S_c}(C(\frac{\partial\rho}{\partial z})\frac{\partial\rho}{\partial z})\vec{n}_z dS&\approx\frac{\Delta xF_0}{P_v}(\mathcal{G}(\frac{\rho_n-\rho_c}{\Delta z})\frac{\rho_n-\rho_c}{\Delta z})-\frac{\Delta xF_0}{P_v}(\mathcal{G}(\frac{\rho_c-\rho_s}{\Delta z})\frac{\rho_c-\rho_s}{\Delta z})\\ \frac{1}{P_v}\int_{S_c}(C(\frac{\partial\rho}{\partial z})\frac{\partial\mu}{\partial z})\vec{n}_z dS&\approx\frac{\Delta xF_0}{P_v}(\mathcal{G}(\frac{\rho_n-\rho_c}{\Delta z})\frac{\mu_n-\mu_c}{\Delta z})-\frac{\Delta xF_0}{P_v}(\mathcal{G}(\frac{\rho_c-\rho_s}{\Delta z})\frac{\mu_c-\mu_s}{\Delta z})\end{aligned}$$

this (incl. boundary conditions) can be represented in matrix form by defining

$$c_n=\begin{bmatrix}0 & & & \\ \frac{1}{\Delta z} & -\frac{1}{\Delta z} & & \\ & \ddots & \ddots & \\ & & \frac{1}{\Delta z} & -\frac{1}{\Delta z}\end{bmatrix},\quad c_s=\begin{bmatrix}\frac{1}{\Delta z} & -\frac{1}{\Delta z} & & \\ & \ddots & \ddots & \\ & & \frac{1}{\Delta z} & -\frac{1}{\Delta z}\\ & & & 0\end{bmatrix}$$

so that

$$C_n:=c_n\otimes I_{nx},\quad C_s=c_s\otimes I_{nx}.$$

Finally rewriting

$$\frac{1}{P_v}\int_{S_i}(C(\frac{\partial\rho}{\partial z})\frac{\partial\rho}{\partial z})\vec{n}_z dS \approx \{\frac{\Delta x F_0}{P_v}(\mathcal{G}(\varepsilon C_n\rho)\odot(C_n\rho)) - \frac{\Delta x F_0}{P_v}(\mathcal{G}(\varepsilon C_s\rho)\odot(C_s\rho))\}_i$$

$$\frac{1}{P_v}\int_{S_i}(C(\frac{\partial\rho}{\partial z})\frac{\partial\mu}{\partial z})\vec{n}_z dS \approx \{\frac{\Delta x F_0}{P_v}(\mathcal{G}(\varepsilon C_n\rho)\odot(C_n\mu)) - \frac{\Delta x F_0}{P_v}(\mathcal{G}(\varepsilon C_s\rho)\odot(C_s\mu))\}_i$$

where $\odot$ denotes the Hadamard (elementwise) product and letting

$$C_N = \begin{bmatrix} C_n & 0 \\ C_n & 0 \end{bmatrix}, \quad C_S = \begin{bmatrix} C_s & 0 \\ C_s & 0 \end{bmatrix}$$

and

$$C_{No} = \begin{bmatrix} C_n & 0 \\ 0 & C_n \end{bmatrix}, \quad C_{So} = \begin{bmatrix} C_s & 0 \\ 0 & C_s \end{bmatrix}$$

the system in compact form now reads

$$M\frac{d}{dt}u = Au + M\overline{u} + C_i(u) \tag{2}$$

where

$$C_1(u) = \frac{\Delta x F_0}{2P_v}((\vec{1}+\tanh(\varepsilon C_N u))\odot(C_{No}u) - (\vec{1}+\tanh(\varepsilon C_S u))\odot(C_{So}u))$$

and

$$C_2(u) = \frac{\Delta x F_0}{P_v}(\max(\vec{0},\tanh^3(C_N u))\odot(C_{No}u) - \max(\vec{0},\tanh^3(C_S u))\odot(C_{So}u))$$

where the $\max(\vec{a},\vec{b})$ is taken elementwise. Finally, note that the continuous integral constraint now translates to

$$\sum_{i=1}^{n_x n_z}\frac{1}{2}(\mu_i-\rho_i) = \sum_{i=1}^{n_x n_z} T_i = 0, \quad \text{if } i_+^{res} - i_-^{res} = 0$$

$$\sum_{i=1}^{n_x n_z}\frac{1}{2}(\rho_i+\mu_i) = \sum_{i=1}^{n_x n_z} S_i = 0, \quad \text{if } i_+^{res} + i_-^{res} = 0.$$

3.3 Linearization

Consider $(\rho,\mu) = (\overline{\rho}+\Delta\rho, \overline{\mu}+\Delta\mu)$ where $(\overline{\rho},\overline{\mu})$ is an equilibrium and $(\Delta\rho,\Delta\mu)$ is an arbitrarily small perturbation. The convective adjustment function can be approximated by a Taylor series around $\frac{\partial\Delta\rho}{\partial z} = 0$, giving

$$C(\frac{\partial\rho}{\partial z}) \approx C(\frac{\partial\overline{\rho}}{\partial z}) + C'(\frac{\partial\overline{\rho}}{\partial z})\frac{\partial\Delta\rho}{\partial z} =: \overline{C} + \overline{C}'\frac{\partial\Delta\rho}{\partial z},$$

where when using $C(\frac{\partial \rho}{\partial z}) = F_0 \mathcal{F}_1(\frac{\partial \rho}{\partial z})$

$$\begin{aligned}\overline{C} &= \frac{F_0}{2}(1 + \tanh(\varepsilon \frac{\partial \overline{\rho}}{\partial z})) \\ \overline{C}' &= \frac{F_0}{2}\varepsilon \operatorname{sech}^2(\varepsilon \frac{\partial \overline{\rho}}{\partial z})\end{aligned}$$

and when using $C(\frac{\partial \rho}{\partial z}) = F_0 \mathcal{F}_2(\frac{\partial \rho}{\partial z})$

$$\begin{aligned}\overline{C} &= F_0 \max(0, \tanh^3(\varepsilon \frac{\partial \overline{\rho}}{\partial z})) \\ \overline{C}' &= F_0 \begin{cases} 3\varepsilon \tanh^2(\varepsilon \frac{\partial \overline{\rho}}{\partial z}) \operatorname{sech}^2(\varepsilon \frac{\partial \overline{\rho}}{\partial z}) & \text{if} \quad \frac{\partial \overline{\rho}}{\partial z} \geq 0 \\ 0 \quad \text{else.} \end{cases}\end{aligned}$$

The convection term in the ρ equation can be expanded out to give:

$$\begin{aligned}(1+C)\frac{\partial}{\partial z}(\overline{\rho} + \Delta\rho) &\approx (1 + \overline{C} + \overline{C}' \frac{\partial \Delta\rho}{\partial z}) \frac{\partial}{\partial z}(\overline{\rho} + \Delta\rho) \\ &= (1+\overline{C})\frac{\partial \overline{\rho}}{\partial z} + (1 + \overline{C} + \overline{C}' \frac{\partial \overline{\rho}}{\partial z})\frac{\partial \Delta\rho}{\partial z} + \overline{C}'(\frac{\partial \Delta\rho}{\partial z})^2 \\ &= (1+\overline{C})\frac{\partial \overline{\rho}}{\partial z} + (1 + \overline{C} + \overline{C}' \frac{\partial \overline{\rho}}{\partial z})\frac{\partial \Delta\rho}{\partial z} + \mathcal{O}((\frac{\partial \Delta\rho}{\partial z})^2).\end{aligned}$$

Doing the same for the μ equation yields:

$$\begin{aligned}(1+C)\frac{\partial}{\partial z}(\overline{\mu} + \Delta\mu) &\approx (1 + \overline{C} + \overline{C}' \frac{\partial \Delta\rho}{\partial z}) \frac{\partial}{\partial z}(\overline{\mu} + \Delta\mu) \\ &= (1+\overline{C})\frac{\partial \overline{\mu}}{\partial z} + (1+\overline{C})\frac{\partial \Delta\mu}{\partial z} + \overline{C}' \frac{\partial \overline{\mu}}{\partial z}\frac{\partial \Delta\rho}{\partial z} + \overline{C}' \frac{\partial \Delta\rho}{\partial z}\frac{\partial \Delta\mu}{\partial z} \\ &= (1+\overline{C})\frac{\partial \overline{\mu}}{\partial z} + (1+\overline{C})\frac{\partial \Delta\mu}{\partial z} + \overline{C}' \frac{\partial \overline{\mu}}{\partial z}\frac{\partial \Delta\rho}{\partial z} + \mathcal{O}(\frac{\partial \Delta\rho}{\partial z}\frac{\partial \Delta\mu}{\partial z}).\end{aligned}$$

Substitution of the above results in system (1) gives

$$\frac{\partial \Delta\rho}{\partial t} = \frac{1}{P_v}\frac{\partial}{\partial z}((1 + \overline{C} + \overline{C}' \frac{\partial \overline{\rho}}{\partial z})\frac{\partial \Delta\rho}{\partial z}) - (i_+^{res}\Delta\rho + i_-^{res}\Delta\mu) + \frac{1}{P_h}\frac{\partial^2 \Delta\rho}{\partial x^2} \tag{3a}$$

$$\frac{\partial \Delta\mu}{\partial t} = \frac{1}{P_v}\frac{\partial}{\partial z}((1+\overline{C})\frac{\partial \Delta\mu}{\partial z} + \overline{C}' \frac{\partial \overline{\mu}}{\partial z}\frac{\partial \Delta\rho}{\partial z}) - (i_-^{res}\Delta\rho + i_+^{res}\Delta\mu) + \frac{1}{P_h}\frac{\partial^2 \Delta\mu}{\partial x^2} \tag{3b}$$

which is the linearized system. System (3) can be compared with the Jacobian matrix of the discretized system, which reads

$$Df(u) = A + C'(u) \tag{4}$$

where when using $\mathcal{F}_1$

$$\begin{aligned}C'(u) = \frac{\Delta x F_0}{2P_v}&((1 + \tanh(\varepsilon C_N u)) \odot C_{No} + ((\varepsilon \operatorname{sech}^2(\varepsilon C_N u) \odot I)C_N) \odot (C_{No}u) \\ &- (1 + \tanh(\varepsilon C_S u)) \odot C_{So} - ((\varepsilon \operatorname{sech}^2(\varepsilon C_S u) \odot I)C_S) \odot (C_{So}u)).\end{aligned}$$

and when using $\mathcal{F}_2$

$$\begin{aligned}C'(u) = \frac{\Delta x F_0}{P_v}&(\max(\vec{0}, \tanh^3(\varepsilon C_N u)) \odot C_{No} \\ &- (\mathcal{H}(C_N u) \odot \tanh^2(\varepsilon C_N u) \odot \operatorname{sech}^2(\varepsilon C_N u)) \odot I \odot (C_{No} u) \\ &- \max(\vec{0}, \tanh^3(\varepsilon C_S u)) \odot C_{So} \\ &+ (\mathcal{H}(C_S u) \odot \tanh^2(\varepsilon C_S u) \odot \operatorname{sech}^2(\varepsilon C_S u)) \odot I \odot (C_{So} u))\end{aligned}$$

where $\mathcal{H}$ is the Heaviside step function which (together with the max(...) function) is taken elementwise.

3.4 Eigenvalue Analysis

3.4.1 Decoupled case

Consider the case $i_-^{res} = 0$, the equations are then decoupled. Assuming a solution of exponential form to (3a), we obtain:

$$\lambda \Delta\rho = \frac{1}{P_v}\frac{\partial}{\partial z}((1 + \overline{C} + \overline{C}'\frac{\partial \overline{\rho}}{\partial z})\frac{\partial \Delta\rho}{\partial z}) - i_+^{res}\Delta\rho + \frac{1}{P_h}\frac{\partial^2 \Delta\rho}{\partial x^2}.$$

For an equilibrium to bifurcate it is necessary that the linear self-adjoint operator

$$\mathcal{L} = \frac{1}{P_v}\frac{\partial}{\partial z}(1 + \overline{C} + \overline{C}'\frac{\partial \overline{\rho}}{\partial z})\frac{\partial}{\partial z} + \frac{1}{P_h}\frac{\partial^2}{\partial x^2} - i_+^{res}$$

be neither positive nor negative definite in the inner product

$$\int_\Omega \hat{f} g d\Omega$$

on a space of functions which have zero flux through the boundary of $\Omega = [0,1] \times [0,1]$. We have

$$\begin{aligned}(\lambda + i_+^{res}) \int_\Omega |\Delta\rho|^2 d\Omega &= \int_\Omega \overline{\Delta\rho}\nabla \cdot \left(\begin{bmatrix} \frac{1}{P_v}(1 + \overline{C} + \overline{C}'\frac{\partial \overline{\rho}}{\partial z}) & 0 \\ 0 & \frac{1}{P_h} \end{bmatrix} \begin{bmatrix} \frac{\partial \Delta\rho}{\partial z} \\ \frac{\partial \Delta\rho}{\partial x} \end{bmatrix} \right) d\Omega \\ &= \int_\Gamma \overline{\Delta\rho} \left(\begin{bmatrix} \frac{1}{P_v}(1 + \overline{C} + \overline{C}'\frac{\partial \overline{\rho}}{\partial z}) & 0 \\ 0 & \frac{1}{P_h} \end{bmatrix} \begin{bmatrix} \frac{\partial \Delta\rho}{\partial z} \\ \frac{\partial \Delta\rho}{\partial x} \end{bmatrix} \right) \cdot \vec{n} d\Gamma \\ &- \int_\Omega \langle \begin{bmatrix} \frac{\partial \overline{\Delta\rho}}{\partial z} \\ \frac{\partial \overline{\Delta\rho}}{\partial x} \end{bmatrix}, \begin{bmatrix} \frac{1}{P_v}(1 + \overline{C} + \overline{C}'\frac{\partial \overline{\rho}}{\partial z}) & 0 \\ 0 & \frac{1}{P_h} \end{bmatrix} \begin{bmatrix} \frac{\partial \Delta\rho}{\partial z} \\ \frac{\partial \Delta\rho}{\partial x} \end{bmatrix} \rangle \Omega \\ &= - \int_\Omega \langle \begin{bmatrix} \frac{\partial \overline{\Delta\rho}}{\partial z} \\ \frac{\partial \overline{\Delta\rho}}{\partial x} \end{bmatrix}, \begin{bmatrix} \frac{1}{P_v}(1 + \overline{C} + \overline{C}'\frac{\partial \overline{\rho}}{\partial z}) & 0 \\ 0 & \frac{1}{P_h} \end{bmatrix} \begin{bmatrix} \frac{\partial \Delta\rho}{\partial z} \\ \frac{\partial \Delta\rho}{\partial x} \end{bmatrix} \rangle d\Omega\end{aligned}$$

where we have used Green's first identity together with the fact that due to zero-flux

$$\int_\Gamma \overline{\Delta\rho} \left(\begin{bmatrix} \frac{1}{P_v}(1 + \overline{C} + \overline{C}'\frac{\partial \overline{\rho}}{\partial z}) & 0 \\ 0 & \frac{1}{P_h} \end{bmatrix} \begin{bmatrix} \frac{\partial \Delta\rho}{\partial z} \\ \frac{\partial \Delta\rho}{\partial x} \end{bmatrix} \right) \cdot \vec{n} d\Gamma = 0.$$

The spectrum of the matrix

$$U = \begin{bmatrix} \frac{1}{P_v}(1 + \overline{C} + \overline{C}' \frac{\partial \overline{\rho}}{\partial z}) & 0 \\ 0 & \frac{1}{P_h} \end{bmatrix}$$

is given by $\sigma(U) = \left\{ \frac{1}{P_v}(1 + \overline{C} + \overline{C}' \frac{\partial \overline{\rho}}{\partial z}), \quad \frac{1}{P_h} \right\}$. The only eigenvalue which may vary in sign is $\lambda_1 = \frac{1}{P_v}(1 + \overline{C} + \overline{C}' \frac{\partial \overline{\rho}}{\partial z})$. The analysis using $\mathcal{F}_1$ is already present in [15], that is: the multiple equilibria (if any) are due to the feedback of self-sustaining diffusion (so spurious). Using $\mathcal{F}_2$ we have that $\overline{C}$ is always non-negative and $\overline{C}'$ is zero when $\frac{\partial \overline{\rho}}{\partial z}$ is negative and positive elsewhere, therefore λ_1 is always positive, and thus $\lambda + i_+^{res} \leq 0$, so $\lambda \leq -i_+^{res}$. Note that $i_+^{res} \in \{0, \frac{1}{2}, 1\}$, so this implies there can be no bifurcations.

3.4.2 Coupled case

We now generalize the inner product to vector valued functions:

$$\int_\Omega \langle \widehat{f}, g \rangle d\Omega.$$

Proceeding analogously as before, we now obtain the equation:

$$\begin{aligned}
\int_\Omega \lambda(|\Delta\rho|^2 + |\Delta\mu|^2) d\Omega = & \int_\Omega \overline{\Delta\rho} \frac{1}{P_v} \frac{\partial}{\partial z}((1 + \overline{C} + \overline{C}' \frac{\partial \overline{\rho}}{\partial z}) \frac{\partial \Delta\rho}{\partial z}) \\
& - \overline{\Delta\rho}(i_+^{res} \Delta\rho + i_-^{res} \Delta\mu) + \overline{\Delta\rho} \frac{1}{P_h} \frac{\partial^2 \Delta\rho}{\partial x^2} \\
& + \overline{\Delta\mu} \frac{1}{P_v} \frac{\partial}{\partial z}((1 + \overline{C}) \frac{\partial \Delta\mu}{\partial z} + \overline{C}' \frac{\partial \overline{\mu}}{\partial z} \frac{\partial \Delta\rho}{\partial z}) \\
& - \overline{\Delta\mu}(i_-^{res} \Delta\rho + i_+^{res} \Delta\mu) + \overline{\Delta\mu} \frac{1}{P_h} \frac{\partial^2 \Delta\mu}{\partial x^2} d\Omega \\
= & \int_\Omega \overline{\Delta\rho} \nabla \cdot (U_\rho \nabla \Delta\rho) + \overline{\Delta\mu} \nabla \cdot (U_\mu \nabla \Delta\mu) \\
& + \overline{\Delta\mu} \nabla \cdot (U_\mu^\rho \Delta\rho) - 2 i_T^{res} |\Delta T|^2 - 2 i_S^{res} |\Delta S|^2 d\Omega
\end{aligned}$$

where

$$\begin{aligned}
U_\rho &= \begin{bmatrix} \frac{1}{P_v}(1 + \overline{C} + \overline{C}' \frac{\partial \overline{\rho}}{\partial z}) & 0 \\ 0 & \frac{1}{P_h} \end{bmatrix} \\
U_\mu &= \begin{bmatrix} \frac{1}{P_v}(1 + \overline{C}) & 0 \\ 0 & \frac{1}{P_h} \end{bmatrix} \\
U_\mu^\rho &= \begin{bmatrix} \frac{1}{P_v} \overline{C}' \frac{\partial \overline{\mu}}{\partial z} & 0 \\ 0 & 0 \end{bmatrix}.
\end{aligned}$$

We can further integrate by parts (most of) the right hand side in the eigenequation to obtain

$$\begin{aligned}\int_\Omega \lambda(|\Delta\rho|^2+|\Delta\mu|^2)d\Omega &= \int_\Gamma (\overline{\Delta\rho}(U_\rho\nabla\Delta\rho)+\overline{\Delta\mu}(U_\mu\nabla\Delta\mu)+\overline{\Delta\mu}(U_\mu^\rho\nabla\Delta\rho))\cdot\vec{n}d\Gamma\\ &-\int_\Omega \langle\nabla\overline{\Delta\rho},U_\rho\nabla\Delta\rho\rangle+\langle\nabla\overline{\Delta\mu},U_\mu\nabla\Delta\mu\rangle+\langle\nabla\overline{\Delta\mu},U_\mu^\rho\nabla\Delta\rho\rangle\\ &+2i_T^{res}|\Delta T|^2+2i_S^{res}|\Delta S|^2d\Omega\\ &=-\int_\Omega\langle\begin{bmatrix}\nabla\overline{\Delta\rho}\\ \nabla\overline{\Delta\mu}\end{bmatrix},\begin{bmatrix}U_\rho & \frac{1}{2}U_\mu^\rho\\ \frac{1}{2}U_\mu^\rho & U_\mu\end{bmatrix}\begin{bmatrix}\nabla\Delta\rho\\ \nabla\Delta\mu\end{bmatrix}\rangle\\ &+2i_T^{res}|\Delta T|^2+2i_S^{res}|\Delta S|^2d\Omega\end{aligned}$$

where again we've used Green's first identity and zero-flux. The determinant of the block matrix in the right hand side of the above equation is given by

$$\det(U)=\frac{1}{P_h^2P_v^2}((1+\overline{C})(1+\overline{C}+\overline{C}'\frac{\partial\overline{\rho}}{\partial z})-(\overline{C}'\frac{\partial\overline{\mu}}{\partial z})^2).$$

The above will be negative if

$$(1+\overline{C})(1+\overline{C}+\overline{C}'\frac{\partial\overline{\rho}}{\partial z})<(\overline{C}'\frac{\partial\overline{\mu}}{\partial z})^2$$

or if

$$(1+\overline{C}+\overline{C}'\frac{\partial\overline{\rho}}{\partial z})<0.$$

When using $\mathcal{F}_1$ both of the above may hold, while when using $\mathcal{F}_2$ only the former condition is possible. The situation where bifurcation occur due to the term $\overline{C}'\frac{\partial\overline{\mu}}{\partial z}$ is called convective feedback [15].

3.5 Numerical Results

3.5.1 Analytical Verification of Numerical Results

We tested the correctness of our numerical approximations by setting $\delta(x)=1$, this returns the original system found in [15] plus x-direction diffusion. Due to the Neumann boundary conditions in the horizontal direction, the solution will in fact be independent of x. Suppose the convective adjustment functions are inactive (we'll soon see this is in fact possible within a certain domain of the parameter space when using $\mathcal{F}_2$), the system in temperature-salinity formulation then reads:

$$\begin{aligned}\frac{\partial T}{\partial t}&=\frac{1}{P_h}\frac{\partial^2T}{\partial x^2}+\frac{1}{P_v}\frac{\partial^2T}{\partial z^2}-(i_T^{res}T-\overline{T}(z))\\ \frac{\partial S}{\partial t}&=\frac{1}{P_h}\frac{\partial^2S}{\partial x^2}+\frac{1}{P_v}\frac{\partial^2S}{\partial z^2}-(i_S^{res}S-\overline{S}(z)).\end{aligned}$$

Where $\overline{T}(z) = \cos(2\pi z)$ and $\overline{S}(z) = \gamma\cos(\pi z)$. To find the steady state solution we first turn to the associated homogeneous system, which is given by the equations:

$$0 = \frac{1}{P_h}\frac{\partial^2 T}{\partial x^2} + \frac{1}{P_v}\frac{\partial^2 T}{\partial z^2} - i_T^{res} T$$
$$0 = \frac{1}{P_h}\frac{\partial^2 S}{\partial x^2} + \frac{1}{P_v}\frac{\partial^2 S}{\partial z^2} - i_S^{res} S.$$

The weak formulation of the temperature problem is given by

$$0 = \int_\Omega \frac{\widehat{T}}{P_h}\frac{\partial^2 T}{\partial x^2} + \frac{\widehat{T}}{P_v}\frac{\partial^2 T}{\partial z^2} - i_T^{res}\widehat{T}T d\Omega = \int_\Omega -\frac{1}{P_h}\frac{\partial T}{\partial x}\frac{\partial \widehat{T}}{\partial x} - \frac{1}{P_v}\frac{\partial T}{\partial z}\frac{\partial \widehat{T}}{\partial z} - i_T^{res}\widehat{T}T d\Omega$$
$$= -(\frac{1}{P_h}\langle\frac{\partial T}{\partial x}, \frac{\partial \widehat{T}}{\partial x}\rangle + \frac{1}{P_v}\langle\frac{\partial T}{\partial z}, \frac{\partial \widehat{T}}{\partial z}\rangle + i_T^{res}\langle T, \widehat{T}\rangle).$$

Since this has to hold for any $\widehat{T}$ it also must hold for $\widehat{T} = T$ and thus we have

$$\frac{1}{P_h}\langle\frac{\partial T}{\partial x}, \frac{\partial T}{\partial x}\rangle + \frac{1}{P_v}\langle\frac{\partial T}{\partial z}, \frac{\partial T}{\partial z}\rangle + i_T^{res}\langle T, T\rangle = 0$$

notive that all the terms in the above equation have the same sign, it then follows that

$$T_{hom}(x,z) = \begin{cases} 0 & \text{if} \quad i_T^{res} \neq 0 \\ \alpha_T & \text{if} \quad i_T^{res} = 0. \end{cases}$$

We can analogously derive that for the salinity

$$S_{hom}(x,z) = \begin{cases} 0 & \text{if} \quad i_S^{res} \neq 0 \\ \alpha_S & \text{if} \quad i_S^{res} = 0. \end{cases}$$

For the particular solution, notice that $\cos(\pi z)$ and $\cos(2\pi z)$ both satisfy the boundary conditions, we then guess a solution of the form

$$T_{part}(x,z) = \beta_T(x)\cos(2\pi z)$$
$$S_{part}(x,z) = \beta_S(x)\cos(\pi z)$$

and upon substitution in the original system's steady state equation we find that

$$\frac{1}{P_h}\beta_T'' - (\frac{4\pi^2}{P_v} + i_T^{res})\beta_T + 1 = 0$$
$$\frac{1}{P_h}\beta_S'' - (\frac{\pi^2}{P_v} + i_S^{res})\beta_S + \gamma = 0$$

which can readily be solved and, after application of the boundary conditions, gives

$$\beta_T(x) = \frac{P_v}{i_T^{res}P_v + 4\pi^2}$$
$$\beta_S(x) = \frac{\gamma P_v}{i_S^{res} + \pi^2}.$$

The analytical solution in the case of zero-convective adjustment ($\frac{\partial \rho}{\partial z} < 0$) is thus given by

$$T(z) = \begin{cases} \frac{P_v \cos(2\pi z)}{i_T^{res} P_v + 4\pi^2} & \text{if} \quad i_T^{res} \neq 0 \\ \frac{P_v \cos(2\pi z)}{4\pi^2} + \alpha_T & \text{else} \end{cases}, \quad S(z) = \begin{cases} \frac{\gamma P_v \cos(\pi z)}{i_S^{res} P_v + \pi^2} & \text{if} \quad i_S^{res} \neq 0 \\ \frac{\gamma P_v \cos(\pi z)}{\pi^2} + \alpha_S & \text{else.} \end{cases}$$

There are two solutions because when $i_S^{res} = 0$ (resp. $i_T^{res} = 0$) the system is underdetermined. The two solutions can in either case be made to coincide by adding the previously used integral constraint, in which case we get

$$T(z) = \frac{P_v \cos(2\pi z)}{i_T^{res} P_v + 4\pi^2}, \quad S(z) = \frac{\gamma P_v \cos(\pi z)}{i_S^{res} P_v + \pi^2}$$

or, in the density-spiciness formulation

$$\rho(z) = \frac{\gamma P_v \cos(\pi z)}{(i_+^{res} + i_-^{res}) P_v + \pi^2} - \frac{P_v \cos(2\pi z)}{(i_+^{res} - i_-^{res}) P_v + 4\pi^2}$$
$$\mu(z) = \frac{\gamma P_v \cos(\pi z)}{(i_+^{res} + i_-^{res}) P_v + \pi^2} + \frac{P_v \cos(2\pi z)}{(i_+^{res} - i_-^{res}) P_v + 4\pi^2}.$$

At this stage it is worth noting that

$$\frac{\partial \rho}{\partial z} = -\frac{\gamma \pi P_v \sin(\pi z)}{(i_+^{res} + i_-^{res}) P_v + \pi^2} + \frac{2\pi P_v \sin(2\pi z)}{(i_+^{res} - i_-^{res}) P_v + 4\pi^2}$$

so we notice that the activation of the convective adjustment depends both on the bifurcation parameter γ *and* on the vertical Peclèt number P_v (the only exception being when $i_T^{res} = i_S^{res} = 0$). In fact, when using $\mathcal{F}_2$ the analytical solution holds in the domain given by

$$\gamma \leq \frac{2(i_+^{res} + i_-^{res}) P_v + \pi^2}{(i_+^{res} - i_-^{res}) P_v + 4\pi^2} \frac{\sin(2\pi z)}{\sin(\pi z)}, \quad \forall \quad z \in [-1, 0].$$

The right hand side obtains its extrema at the boundaries, in particular its minimum is located at $z = -1$ where

$$\frac{2\pi \cos(-2\pi)}{\pi \cos(-\pi)} = -2,$$

thus the validity of the analytical solution (when using $\mathcal{F}_2$) is restricted to the domain

$$\gamma \leq -2 \frac{2(i_+^{res} + i_-^{res}) P_v + \pi^2}{(i_+^{res} - i_-^{res}) P_v + 4\pi^2}.$$

With all of this information at hand we can check the correctness of our numerical solutions by comparing them with the analytical solution (see figure 2). Note that we should expect second order convergence, which is indeed reflected in figure 3. A further confirmation that everything is in fact correct comes from repeating a bifurcation diagram given in [15] for $\mathcal{F}_2$, see figure 4.

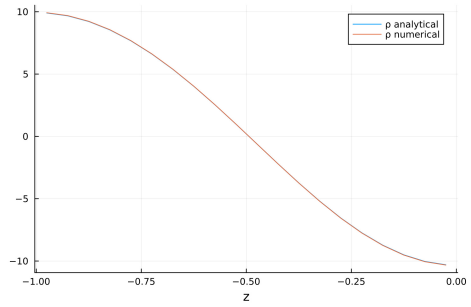

Figure 2: Analytical and numerical solutions for $\gamma = -10$ and $P_v = 10$, using $\mathcal{F}_2$.

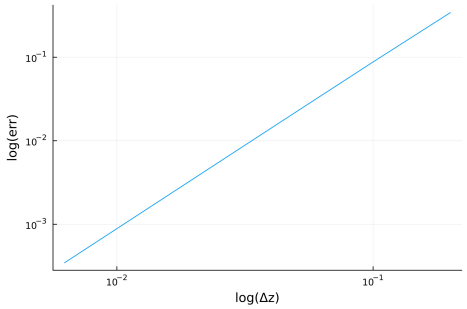

Figure 3: Log plot of the (true) error behaviour for $\gamma = -10$ and $P_v = 10$, using $\mathcal{F}_2$.

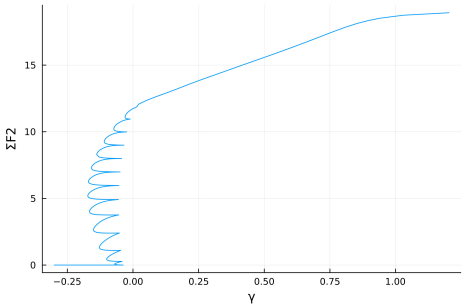

Figure 4: A bifurcation diagram for the coupled modified den Toom system (no x-heterogeneity), using $\mathcal{F}_2$. This structure is also present in the one-dimensional version of the system, treated in [15]. Here $P_v = 10^3$, $n_x = 5$ and $n_z = 20$. Note that the summation was performed only over the vertical direction.

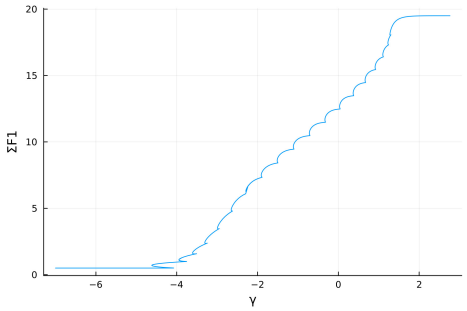

Figure 5: A bifurcation diagram for the uncoupled modified den Toom system (no x-heterogeneity), using $\mathcal{F}_1$. This structure, although present in the one-dimensional system, is not shown in [15]. Here $P_v = 10^3$, $n_x = 5$ and $n_z = 20$. Note that the summation was performed only over the vertical direction.

3.5.2 Numerical Results when using $\mathcal{F}_1$

Throughout this subsubsection we treat the decoupled system (i.e. $i_-^{res} = 0$) with $n_x = n_z = 10$ and as specified in section 2.1 we will use $\delta(x) = \cos(\frac{\pi x}{2})$. Numerical continuation for a value of $P_v = 1$ (small enough that no bifurcations occur in the one dimensional system), reveals that in fact the addition of horizontal spatial heterogeneity and diffusion causes no new bifurcations to occur, in spite of how large P_h is made. This is shown in figure 6.

However when one increases P_v to 10^3, for $P_h = 1$ horizontal diffusion acts as a smoothing factor: the bifurcations that would otherwise be present in the one dimensional

model disappear and are instead replaced by sudden near-discontinuities (these are in fact not proper discontinuities, in spite of appearing as such). See figure 7 for a comparison of these scenarios.

Finally, using $P_h = 100$ and as before $P_v = 10^3$ we do observe some fragmented tipping (see figures 8-9).

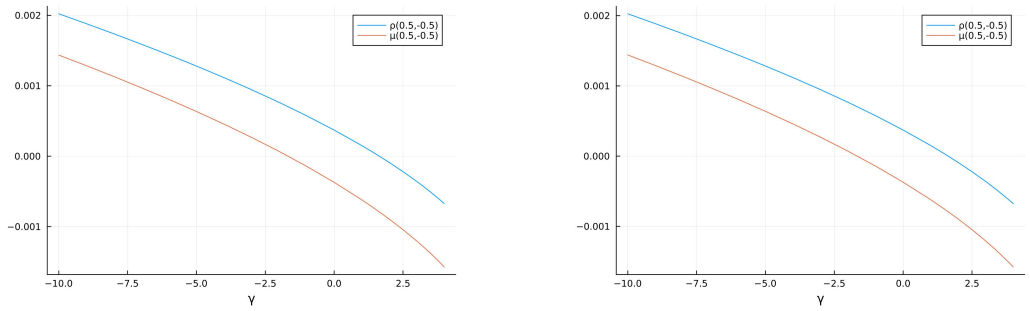

Figure 6: Bifurcation diagram for $P_v = 1 = P_h$ (left) and $P_v = 1$, $P_h = 10^3$ (right). The plot shows the values of both ρ and μ in the center of the domain (i.e. at $x = -z = \frac{1}{2}$). Notice the absence of bifurcations, this tells us that horizontal spatial heterogeneity and diffusion alone creates no new bifurcations.

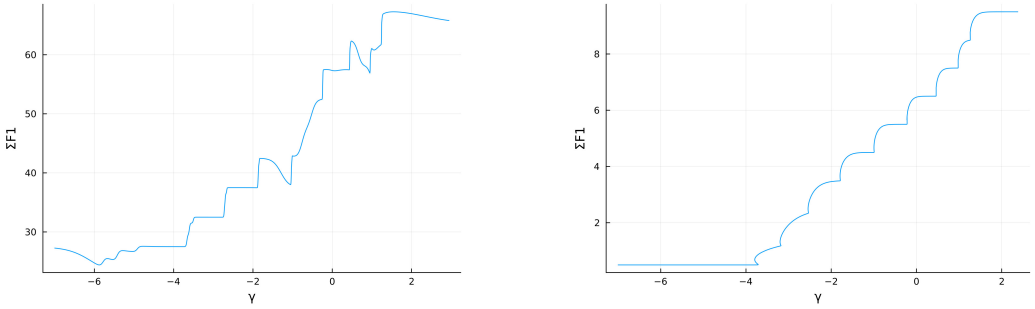

Figure 7: Bifurcation diagrams with $P_h = 1$, $P_v = 10^3$ and $n_x = n_z = 10$. The left hand side plot has horizontal spatial heterogeneity, while the right hand side one doesn't. It is evident that in this scenario the horizontal spatial heterogeneity acts as a damping, preventing bifurcations from occuring.

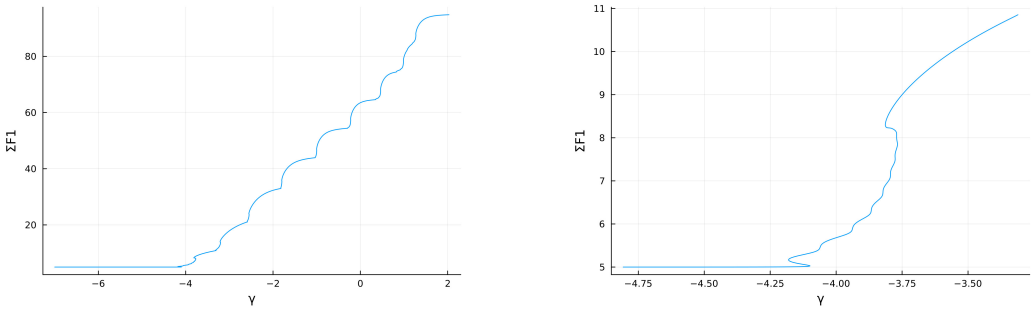

Figure 8: Bifurcation diagram with $P_h = 100$ and $P_v = 10^3$ with horizontal spatial heterogeneity (left). Detail of the first (fragmented) fold of the left hand side bifurcation diagram (right). The latter can be compared with figure 9.

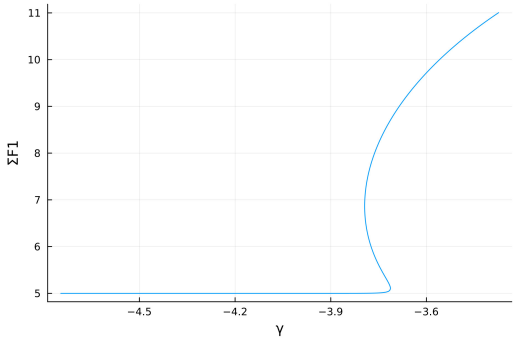

Figure 9: Detail of the first (leftmost) fold in the right hand side plot of figure 7 (i.e. for a system with no horizontal spatial heterogeneity and $P_v = 10^3$). Note that we multiply the summation by 10 due to the fact that we are comparing with a summation over the entire domain rather than just the vertical dimension.

3.5.3 Numerical Results when using $\mathcal{F}_2$

In the coupled system ($i_+^{res} = -i_-^{res} = \frac{1}{2}$) when using $\mathcal{F}_2$, upon fixing $P_v = 1$ we again observe the same results as for the decoupled system, that is: the addition of horizontal spatial heterogeneity and diffusion results in no new bifurcations. See figure 10.

Setting $P_h = 1$ and subsequently $P_h = 50$ we repeat the continuation with $n_x = n_z = 10$ see figures 11 and 12. While the horizontal Peclet number is small, we get the same bifurcation diagram (qualitatively) as in [15] (the number of back to back folds again depends on the number of grid points), however we also notice that when the horizontal Peclet number is large enough, a number of new bifurcations occur between the pre-existing bifurcations. These may be spurious or they may be fragmented tipping, however the key argument for the spuriousness of the bifurcations seen in figures 4 and 11 is the dependence of their number on the number of grid points. We see no clear pattern in the exact number of bifurcations between the pre-existing bifurcations, thus leading us to

believe that this is in fact fragmented tipping.

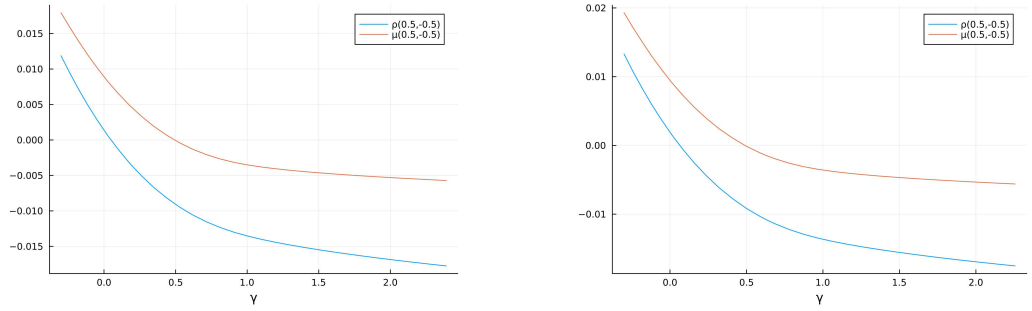

Figure 10: Bifurcation diagram for the coupled system with horizontal spatial heterogeneity using $P_v = 1$, $P_h = 1$ (left) and $P_h = 10^3$ (right). Again this shows that no bifurcations are caused by the simple addition of horizontal spatial heterogeneity and diffusion.

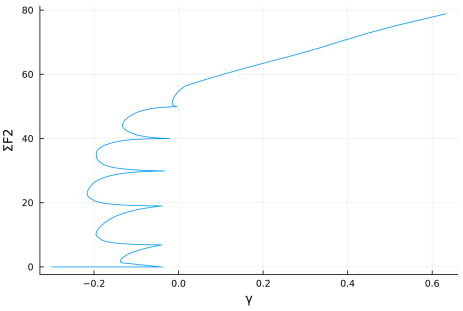

Figure 11: Bifurcation diagram for the coupled system, using $n_x = n_z = 10$, $P_h = 1$ and $P_v = 10^3$. We notice no qualitative difference from the one-dimensional case [15].

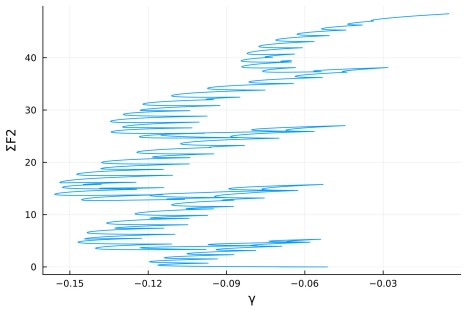

Figure 12: Bifurcation diagram for the coupled system, using $n_x = n_z = 10$, $P_h = 50$ and $P_v = 10^3$. Notice the appearance of several new folds between the ones in figure 11.

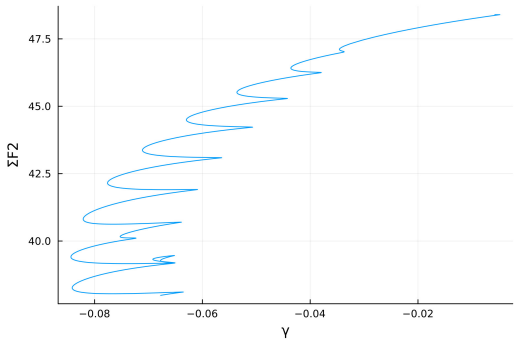

Figure 13: Detail of the bifurcations occurring in figure 12 between the first and third folds (starting from the top) in figure 11.

3.5.4 Discussion

We have seen that both the coupled and decoupled den Toom systems can exhibit fragmented tipping under appropriate choices of diffusion coefficients, when horizontal spatial heterogeneity and diffusion is added to the system. This tells us that if any one pair of fold bifurcations in either system are non-spurious, then we can expect non-spurious fragmented tipping to occur. This would then suggest that the multiple equilibria which are found in e.g. the Veros global ocean model [11], would then also be non-spurious. It just so happens that there is a model due to Bastiaansen [1], which has non-spurious multiple equilibria. We will study a modification of this model in the next section.

4 Modified Bastiaansen model

In a recent article [1], Bastiaansen et al. propose a model for thermohaline circulation based on a simpler ODE model due to Welander [17]. The model is derived starting from the equations:

$$\frac{\partial T}{\partial t} = D_h \frac{\partial^2 T}{\partial x^2} + k_T(T_A(x) - T) - \kappa(\Delta\rho)(T - T_0(x))$$
$$\frac{\partial S}{\partial t} = D_h \frac{\partial^2 S}{\partial x^2} + k_S(S_A(x) - S) - \kappa(\Delta\rho)(S - S_0(x)).$$

Where T and S are now the temperature and salinity of the mid ocean, while T_A (resp. S_A) represent the temperature (resp. salinity) of the atmosphere and T_0 (resp. S_0) represent the temperature and salinity of the deep ocean. In the article, the function representing the rate of exchange with the deep ocean used is

$$\kappa(\Delta\rho) = \frac{\overline{\kappa}}{2}(1 + \tanh(\Delta\rho - \frac{1}{2}))$$

where $\overline{\kappa} = 100$. The system is then expressed in terms of $\Delta T = T - T_0$ and $\Delta S = S - S_0$, and subsequently subtracted (resp. added) to obtain a system in terms of $\Delta\rho = \rho - \rho_0$

(resp. $\Delta\mu = \mu - \mu_0$). We instead perform the subtraction and addition only, obtaining

$$\frac{\partial \rho}{\partial t} = D_h \frac{\partial^2 \rho}{\partial x^2} + k_\rho(\rho_A(x) - \rho) - \kappa(\rho - \rho_0)(\rho - \rho_0(x))$$
$$\frac{\partial \mu}{\partial t} = D_h \frac{\partial^2 \mu}{\partial x^2} + k_\mu(\mu_A(x) - \mu) - \kappa(\rho - \rho_0)(\mu - \mu_0(x)).$$

Next we discard the spiciness equation, and notice that when introducing a three-point vertical grid, the non-diffusive terms in the density equation can in fact be rewritten as

$$\begin{aligned} k_\rho(\rho_A(x) - \rho) - \kappa(\rho - \rho_0)(\rho - \rho_0(x)) &= \Delta z[k_\rho(\frac{\rho_A(x) - \rho}{\Delta z}) - \kappa(\frac{\rho - \rho_0}{\Delta z}\Delta z)(\frac{\rho - \rho_0(x)}{\Delta z})] \\ &\approx \Delta z \tilde{D}_v \frac{\partial}{\partial z}(\kappa(\frac{\partial \rho}{\partial z}\Delta z)\frac{\partial \rho}{\partial z}) =: D_v \frac{\partial}{\partial z}(C(\frac{\partial \rho}{\partial z})\frac{\partial \rho}{\partial z}) \end{aligned}$$

where the vertical diffusion coefficient $D_v = \tilde{D}_v \Delta z = \Delta z$ and using the boundary conditions

$$C(\frac{\partial \rho}{\partial z})\frac{\partial \rho}{\partial z}\Big|_{z=0} = k_\rho(\rho_A(x) - \rho)\Big|_{z=0}, \quad \rho\Big|_{z=-1} = \rho_0(x).$$

We thus rewrite the equation as

$$\frac{\partial \rho}{\partial t} = \frac{1}{P_v}\frac{\partial}{\partial z}(C(\frac{\partial \rho}{\partial z})\frac{\partial \rho}{\partial z}) + \frac{1}{P_h}\frac{\partial^2 \rho}{\partial x^2}$$

where we have relabelled $D_h = \frac{1}{P_h}$ and $D_v = \frac{1}{P_v}$, and notice finally that in fact we obtained the same system as the modified den Toom system, except for the spatial heterogeneity term, with $i_+^{res} = 0$ and with zero z-diffusion. We thus add these back into the equation and obtain the full model:

$$\frac{\partial \rho}{\partial t} = \frac{1}{P_v}\frac{\partial}{\partial z}(i_\Delta^{res} + C(\frac{\partial \rho}{\partial z})\frac{\partial \rho}{\partial z}) - (i_+^{res}\rho - \overline{\rho}(z)) + \frac{1}{P_h}\frac{\partial^2 \rho}{\partial x^2} \tag{5}$$

where $i_\Delta^{res} \in \{0, 1\}$. This system is nearly identical to the uncoupled system of the previous section, but now with boundary conditions given by

$$\begin{aligned} \frac{\partial \rho(x = -1, z)}{\partial x} &= \frac{\partial \rho(x = 1, z)}{\partial x} = 0 \\ C(\frac{\partial \rho(x, z = 0)}{\partial z})\frac{\partial \rho(x, z = 0)}{\partial z} &= k_\rho(\rho_A(x) - \rho(x, z = 0)) \\ \rho(x, z = -1) &= \rho_0(x) \end{aligned}$$

Similarly to what was done in the previous section (resp. in [1]) we take

$$\begin{aligned} \rho_0(x) &= 0 \\ \overline{\rho}(z) &= \delta^{res}(\gamma_1 \cos(\pi z) - \cos(2\pi z)) \\ \rho_A(x) &= \frac{1}{2}(2 + \gamma_2(1 + \cos(\frac{\pi x}{2}))). \end{aligned}$$

where also $\delta^{res} \in \{0, 1\}$ now serves merely as a means to remove the den Toom spatial heterogeneity from the system.

4.1 Discretization

It may at first seem unnecessary to provide a discretization of equation (5) as we derived this from a "discretized" system, however it is worth noting that what we have so far interpreted as a discretization is a very rough one. As in the previous section we will again first consider the system without convective adjustment and discretise the convective adjustment separately. We will also use a non-uniformly spaced grid, since conceptually this resembles the Bastiaansen system more closely. The grid will be stretched via the map

$$\xi(z) = -\frac{e^{-\alpha z} - 1}{e^{\alpha} - 1}$$

(recall that $z \in [-1, 0]$). One can easily check that in fact $\xi(0) = 0$ and $\xi(-1) = -1$. The parameter α, responsible for the intensity of the stretching will henceforth be referred to as the *stretching factor*.

4.1.1 Without Convective Adjustment

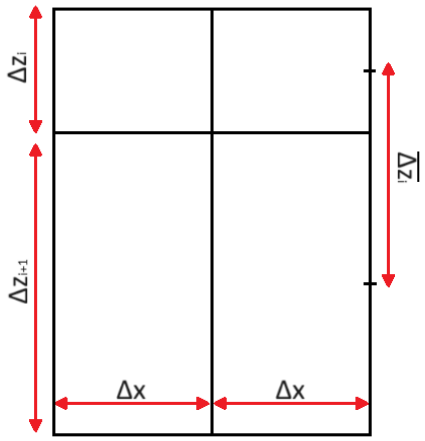

Figure 14: An example of the type of stretched grid used in the discretization. The vertical volume contribution to the horizontal discretization is labelled $\overline{\Delta z}_i$, the vertical volume contribution to the vertical discretization is labelled Δz_i while the horizontal contribution is equal in both cases and labelled Δx.

In absence of convective adjustment, system (5) reads

$$\frac{\partial \rho}{\partial t} = \frac{i_{\Delta}^{res}}{P_v}\frac{\partial^2 \rho}{\partial z^2} - (i_{+}^{res}\rho - \overline{\rho}(z)) + \frac{1}{P_h}\frac{\partial^2 \rho}{\partial x^2}.$$

Again using the Gauss theorem one obtains

$$\iint \frac{i_\Delta^{res}}{P_v}\frac{\partial^2\rho}{\partial z^2} - (i_+^{res}\rho - \overline{\rho}(z)) + \frac{1}{P_h}\frac{\partial^2\rho}{\partial x^2}dV = \int (\frac{i_\Delta^{res}}{P_v}\frac{\partial\rho}{\partial z} + \frac{1}{P_h}\frac{\partial\rho}{\partial x}) \cdot \vec{n}dS - \iint (i_+^{res}\rho - \overline{\rho}(z))dV$$

which can be discretized giving

$$\int_{S_c} (\frac{i_\Delta^{res}}{P_v}\frac{\partial\rho}{\partial z} + \frac{1}{P_h}\frac{\partial\rho}{\partial x}) \cdot \vec{n}dS - \iint_{V_c} (i_+^{res} - \overline{\rho}(z))dV \approx$$
$$i_\Delta^{res}\frac{\Delta x}{P_v}(\frac{\rho_n - \rho_c}{\Delta z_n} - \frac{\rho_c - \rho_s}{\Delta z_s}) + \frac{\overline{\Delta z}_c}{P_h}(\frac{\rho_e - \rho_c}{\Delta x} - \frac{\rho_e - \rho_c}{\Delta x}) - (i_+^{res}\rho_c - \overline{\rho}(z_c))\Delta x\overline{\Delta z}_c$$

where we choose a non-uniform grid in the z-direction and $\overline{\Delta z_c} = \frac{1}{2}(\Delta z_n + \Delta z_s)$. The matrices are then

$$D_x = \begin{bmatrix} -\frac{1}{P_h\Delta x} & \frac{1}{\Delta x P_h} & & & \\ \frac{1}{\Delta x P_h} & -\frac{2}{\Delta x P_h} & \frac{1}{\Delta x P_h} & & \\ & \ddots & \ddots & \ddots & \\ & & \frac{1}{\Delta x P_h} & -\frac{2}{\Delta x P_h} & \frac{1}{\Delta x P_h} \\ & & & \frac{1}{\Delta x P_h} & -\frac{1}{\Delta x P_h} \end{bmatrix} \in \mathbb{R}^{nx\times nx}$$

where we have used that along the horizontal boundaries $\frac{\partial\rho}{\partial x} = 0 \implies \rho_e = \rho_c = \rho_w$, and

$$D_z = i_\Delta^{res}\begin{bmatrix} d_1 & \frac{\Delta x}{\Delta z_1 P_v} & & & \\ \frac{\Delta x}{\Delta z_1 P_v} & d_2 & \frac{\Delta x}{\Delta z_2 P_v} & & \\ & \ddots & \ddots & \ddots & \\ & & \frac{\Delta x}{\Delta z_{nz-2} P_v} & d_{nz-1}\frac{\Delta x}{\Delta z_{nz-1} P_v} & \\ & & & \frac{\Delta x}{\Delta z_{nz-1} P_v} & d_{nz} \end{bmatrix} \in \mathbb{R}^{nz\times nz}$$

with $d_i = (-\frac{\Delta x}{P_v\Delta z_{i-1}} - \frac{\Delta x}{P_v\Delta z_i})$, $d_{nz} = (-\frac{\Delta x}{P_v\Delta z_{nz-1}} - \frac{2\Delta x}{P_v\Delta z_{nz}})$ and where we have used that at the south boundary $\rho = 0 \implies \frac{\rho_c+\rho_s}{2} = 0 \implies \rho_s = -\rho_c$. We left the north boundary condition out as it is nonlinear, this will be added later as an equation to the system. Again the discretized Laplacian is then

$$\tilde{L} = (\overline{\Delta z} \odot I_{nz}) \otimes D_x + D_z \otimes I_{nx}.$$

In order to include the north face's boundary conditions we define

$$i_N^0 = \begin{bmatrix} 1 & 0 & \dots & 0 \\ 0 & 0 & & \vdots \\ \vdots & & \ddots & 0 \\ 0 & \dots & 0 & 0 \end{bmatrix}, \quad i_N^1 = \begin{bmatrix} 0 & 0 & \dots & 0 \\ 0 & 1 & & \vdots \\ \vdots & & \ddots & 0 \\ 0 & \dots & 0 & 1 \end{bmatrix}$$

so that

$$I_N^0 = i_N^0 \otimes I_{nx}, \quad I_N^1 = i_N^1 \otimes I_{nx}.$$

Finally redefining

$$L = I_N^1 \cdot \tilde{L}$$

the discretized system without the convective adjustment and in absence of the northern boundary condition then reads

$$\Delta x \overline{\Delta Z} \frac{d}{dt}\rho = L\rho - (I_N^1 \odot \overline{\Delta z}\Delta x)(i_+^{res}\rho + \overline{\rho}).$$

with $\overline{\Delta Z} = (\overline{\Delta z} \odot I_{nz}) \otimes I_{nx}$.

4.1.2 Discretization of the Convective Adjustment

Again as for the modified den Toom system we note that

$$\iint \frac{1}{P_v}\frac{\partial}{\partial z}(C(\frac{\partial \rho}{\partial z})\frac{\partial \rho}{\partial z})dV = \int \frac{1}{P_v} C(\frac{\partial \rho}{\partial z})\frac{\partial \rho}{\partial z} dS$$

which we can discretize again as

$$\begin{aligned}
&\frac{1}{P_v}\int_{S_c} C(\frac{\partial \rho}{\partial z})\frac{\partial \rho}{\partial z} dS \approx \frac{\Delta x}{P_v}(C(\frac{\rho_n - \rho_c}{\Delta z_n})\frac{\rho_n - \rho_c}{\Delta z_n} - C(\frac{\rho_c - \rho_s}{\Delta z_s})\frac{\rho_c - \rho_s}{\Delta z_s}) \\
=&\frac{\overline{\kappa}\Delta x}{2P_v}((1 + \tanh(\frac{\rho_n - \rho_c}{\Delta z_n} - \frac{1}{2}))\frac{\rho_n - \rho_c}{\Delta z_n} - (1 + \tanh(\frac{\rho_c - \rho_s}{\Delta z_s} - \frac{1}{2}))\frac{\rho_c - \rho_s}{\Delta z_s}).
\end{aligned}$$

Ignoring the north boundary condition and again using that at the southern boundary $\frac{\rho_c + \rho_s}{2} = 0 \implies \rho_c = -\rho_s$, we define the matrices

$$c_n = \begin{bmatrix} -\frac{1}{\Delta z_0} & & & \\ \frac{1}{\Delta z_1} & -\frac{1}{\Delta z_1} & & \\ & \ddots & \ddots & \\ & & \frac{1}{\Delta z_{nz-1}} & -\frac{1}{\Delta z_{nz-1}} \end{bmatrix}, \quad c_s = \begin{bmatrix} \frac{1}{\Delta z_1} & -\frac{1}{\Delta z_1} & & \\ & \ddots & \ddots & \\ & & \frac{1}{\Delta z_{nz-1}} & -\frac{1}{\Delta z_{nz-1}} \\ & & & \frac{2}{\Delta z_{nz}} \end{bmatrix}$$

so that

$$C_n = c_n \otimes I_{nx}, \quad C_s = c_s \otimes I_{nx}.$$

Finally define

$$\begin{aligned}
\tilde{K}(\rho) &= \frac{\Delta x \overline{\kappa}}{2P_v}((\vec{1} + \tanh(C_n\rho - \frac{1}{2}\vec{1})) \odot (C_n\rho) - (\vec{1} + \tanh(C_s\rho - \frac{1}{2}\vec{1})) \odot (C_s\rho)) \\
K(\rho) &= I_N^1 \cdot \tilde{K}(\rho).
\end{aligned}$$

As for the north boundary condition, at each point in the x direction, this can be written as

$$k_\rho(\rho_A(x_c) - \frac{\rho_n + \rho_c}{2}) - \frac{\overline{\kappa}}{2}(1 + \tanh(\frac{\rho_n - \rho_c}{\Delta z_0} - \frac{1}{2}))\frac{\rho_n - \rho_c}{\Delta z_0} = 0$$

so, defining

$$c_{avg} = \begin{bmatrix} \frac{1}{2} & \frac{1}{2} & & & \\ & 0 & 0 & & \\ & & \ddots & \ddots & \\ & & & 0 & 0 \\ & & & & 0 \end{bmatrix} \in \mathbb{R}^{nz \times nz}, \quad C_{avg} = c_{avg} \otimes I_{nx}$$

in matrix form this would translate to

$$k_\rho(\rho_A(x) - C_{avg}\rho) - \frac{\overline{\kappa}}{2}(\vec{1} + \tanh(C_n\rho - \frac{1}{2}\vec{1})) \odot (C_n\rho) = 0$$

where clearly now $\rho_A(x) = (\rho_A(x_1), \ldots, \rho_A(x_{nx}), 0, \ldots, 0)^T$. Define

$$N(\rho) = k_\rho(\rho_A(x) - C_{avg}\rho) - \frac{\overline{\kappa}}{2} I_N^0(\vec{1} + \tanh(C_s\rho - \frac{1}{2}\vec{1})) \odot (C_s\rho),$$

then the system in matrix form is given by

$$M\frac{d}{dt}\rho = L\rho - I_N^1 \Delta x \overline{\Delta Z}(i_+^{res}\rho + \overline{\rho}) + K(\rho) + N(\rho)$$

where the mass matrix is now

$$M = \begin{bmatrix} 0 & 0 \\ 0 & I_{(nx-1)\cdot(nz-1)} \end{bmatrix} \Delta x \overline{\Delta Z}.$$

The discrete Jacobian matrix is now

$$Df(\rho) = L - I_N^1 \Delta x \overline{\Delta Z} i_+^{res} + K'(\rho) + N'(\rho)$$

where

$$\begin{aligned} K'(\rho) = I_N^1 \frac{\Delta x \overline{\kappa}}{2P_v}((\vec{1} + \tanh(C_n\rho - \frac{1}{2}\vec{1})) \odot C_n + (\operatorname{sech}^2(C_n\rho - \frac{1}{2}\vec{1}) \odot C_n) \odot (C_n\rho) \\ - (\vec{1} + \tanh(C_s\rho - \frac{1}{2})) \odot C_s - (\operatorname{sech}^2(C_s\rho - \frac{1}{2}\vec{1}) \odot C_s) \odot (C_s\rho)) \end{aligned}$$

and

$$\begin{aligned} N'(\rho) = -k_\rho C_{avg} - \frac{\overline{\kappa}}{2} I_N^0((\vec{1} + \tanh(C_s\rho - \frac{1}{2}\vec{1})) \odot C_s \\ + (\operatorname{sech}^2(C_n\rho - \frac{1}{2}\vec{1}) \odot C_s) \odot (C_s\rho)). \end{aligned}$$

4.2 Linearization and Eigenvalue Analysis

Repeating the analogous steps as in section 2.2, we may obtain the linearized system as

$$\frac{\partial \Delta\rho}{\partial t} = \frac{1}{P_v}\frac{\partial}{\partial z}((i_\Delta^{res} + \overline{C} + \overline{C}'\frac{\partial \overline{\rho}}{\partial z})\frac{\partial \Delta\rho}{\partial z}) - i_+^{res}\Delta\rho + \frac{1}{P_h}\frac{\partial^2 \Delta\rho}{\partial x^2}.$$

The boundary conditions however are different now, at the south boundary

$$\overline{\rho} + \Delta\rho\Big|_{z=-1} = 0$$

so that

$$\Delta\rho\Big|_{z=-1} = 0,$$

while at the north boundary we have that

$$\begin{aligned} C(\frac{\partial\overline{\rho}}{\partial z} + \frac{\partial\Delta\rho}{\partial z})(\frac{\partial\overline{\rho}}{\partial z} + \frac{\partial\Delta\rho}{\partial z})\Big|_{z=0} &= \overline{C}\frac{\partial\overline{\rho}}{\partial z} + (\overline{C} + \overline{C}'\frac{\partial\overline{\rho}}{\partial z})\frac{\partial\Delta\rho}{\partial z}\Big|_{z=0} \\ &= k_\rho(\rho_A(x) - \overline{\rho}) - k_\rho\Delta\rho\Big|_{z=0} \end{aligned}$$

so that

$$(\overline{C} + \overline{C}'\frac{\partial\overline{\rho}}{\partial z})\frac{\partial\Delta\rho}{\partial z}\Big|_{z=0} = -k_\rho\Delta\rho\Big|_{z=0}, \quad \Longrightarrow \quad \frac{\partial\Delta\rho}{\partial z}\Big|_{z=0} = \frac{-k_\rho\Delta\rho}{\overline{C} + \overline{C}'\frac{\partial\overline{\rho}}{\partial z}}\Big|_{z=0}$$

(recall in particular that $k_\rho = 1$). Similarly to what was done for the modified den Toom system we again assume a solution of exponential form and check definiteness of the linear self-adjoint operator

$$\mathcal{L} = \frac{1}{P_v}\frac{\partial}{\partial z}(i_\Delta^{res} + \overline{C} + \overline{C}'\frac{\partial\overline{\rho}}{\partial z})\frac{\partial}{\partial z} + \frac{1}{P_h}\frac{\partial^2}{\partial x^2} - i_+^{res}$$

under the inner product $\int_\Omega \widehat{f}g d\Omega$ on a space of functions which now have zero-flux boundary conditions in the horizontal direction and the above boundary conditions in the vertical direction. We then have

$$\begin{aligned} (\lambda + i_+^{res})\int_\Omega |\Delta\rho|^2\, d\Omega &= \int_\Omega \overline{\Delta\rho}\nabla\cdot\left(\begin{bmatrix} \frac{1}{P_v}(i_\Delta^{res} + \overline{C} + \overline{C}'\frac{\partial\overline{\rho}}{\partial z}) & 0 \\ 0 & \frac{1}{P_h}\end{bmatrix}\begin{bmatrix}\frac{\partial\Delta\rho}{\partial z} \\ \frac{\partial\Delta\rho}{\partial x}\end{bmatrix}\right) d\Omega \\ &= \int_\Gamma \overline{\Delta\rho}\left(\begin{bmatrix} \frac{1}{P_v}(i_\Delta^{res} + \overline{C} + \overline{C}'\frac{\partial\overline{\rho}}{\partial z}) & 0 \\ 0 & \frac{1}{P_h}\end{bmatrix}\begin{bmatrix}\frac{\partial\Delta\rho}{\partial z} \\ \frac{\partial\Delta\rho}{\partial x}\end{bmatrix}\right)\cdot\vec{n}d\Gamma \\ &- \int_\Omega\left(\begin{bmatrix} \frac{1}{P_v}(i_\Delta^{res} + \overline{C} + \overline{C}'\frac{\partial\overline{\rho}}{\partial z}) & 0 \\ 0 & \frac{1}{P_h}\end{bmatrix}\begin{bmatrix}\frac{\partial\Delta\rho}{\partial z} \\ \frac{\partial\Delta\rho}{\partial x}\end{bmatrix}\right)\cdot\begin{bmatrix}\frac{\partial\overline{\Delta\rho}}{\partial z} \\ \frac{\partial\overline{\Delta\rho}}{\partial x}\end{bmatrix} d\Omega \\ &= -\frac{1}{P_v}\frac{(i_\Delta^{res} + \overline{C} + \overline{C}'\frac{\partial\overline{\rho}(x,0)}{\partial z})}{(\overline{C} + \overline{C}'\frac{\partial\overline{\rho}(x,0)}{\partial z})}|\Delta\rho(x,0)|^2 \\ &- \int_\Omega\left(\begin{bmatrix} \frac{1}{P_v}(i_\Delta^{res} + \overline{C} + \overline{C}'\frac{\partial\overline{\rho}}{\partial z}) & 0 \\ 0 & \frac{1}{P_h}\end{bmatrix}\begin{bmatrix}\frac{\partial\Delta\rho}{\partial z} \\ \frac{\partial\Delta\rho}{\partial x}\end{bmatrix}\right)\cdot\begin{bmatrix}\frac{\partial\overline{\Delta\rho}}{\partial z} \\ \frac{\partial\overline{\Delta\rho}}{\partial x}\end{bmatrix} d\Omega. \end{aligned}$$

The mechanism which is responsible for any potentially new bifurcations is thus again self sustaining diffusion. Notice that in this case the choice of i_Δ^{res} is nontrivial: if $i_\Delta^{res} = 0$ we should expect more or less the same structure as seen in the decoupled den Toom system, whereas if $i_\Delta^{res} = 1$ the self sustaining diffusion can cause new bifurcations to appear, due to the north boundary condition term.

4.3 Numerical Results

Using γ_2 as continuation parameter, we first perform the continuation on an unstretched grid. Again we notice that the exact number of back to back fold bifurcations depends on the number of grid points. In this case the dependence is in the horizontal rather than the vertical direction. See figures 15-17.

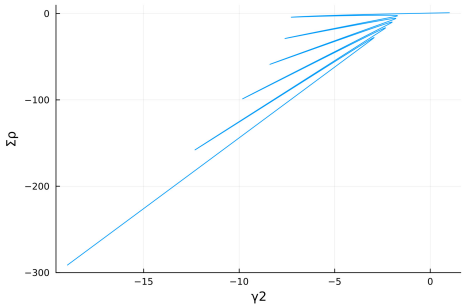

Figure 15: Bifurcation diagram for the modified Bastiaansen system using 10 points in the horizontal direction and 3 points in the vertical direction.

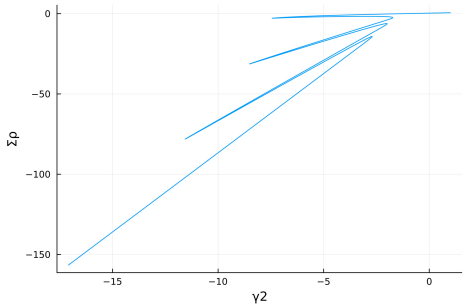

Figure 16: Bifurcation diagram for the modified Bastiaansen system using 6 points in the horizontal direction and 3 points in the vertical direction.

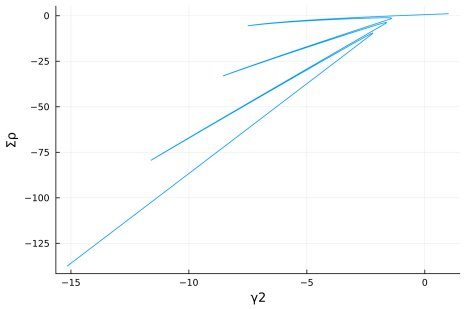

Figure 17: Bifurcation diagram for the modified Bastiaansen system using 6 points in the horizontal direction and 6 points in the vertical direction.

Next, we fix the number of gridpoints to $n_x = 6$, and $n_z = 3$ for ease of continuation, we then stretch the grid to see if this is of any help in obtaining a bifurcation diagram more similar to that found in [1]. See figures 18-21. Observe that the greater the stretching factor the closer the equilibrium curves become, however they don't exactly approach the bifurcation diagram we were looking for and this ends up making the continuation unnecessarily difficult: the Newton iterations in the Moore Penrose scheme take a much longer time to converge due to the closeness of other equilibria. The opposite is true when

the stretching factor is taken to be very negative. Either way, stretching the grid does not seem to have a qualitative effect on the system.

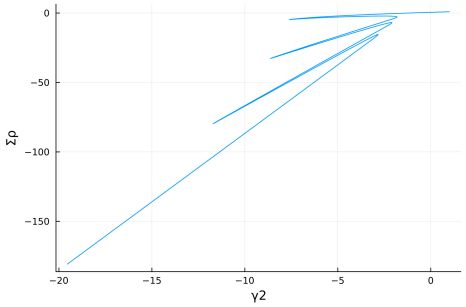

Figure 18: Bifurcation diagram for the modified Bastiaansen system using a grid stretched by a factor of 1.

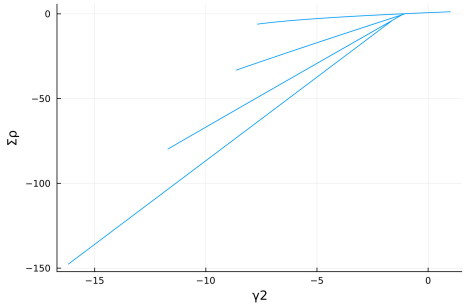

Figure 19: Bifurcation diagram for the modified Bastiaansen system using a grid stretched by a factor of 10.

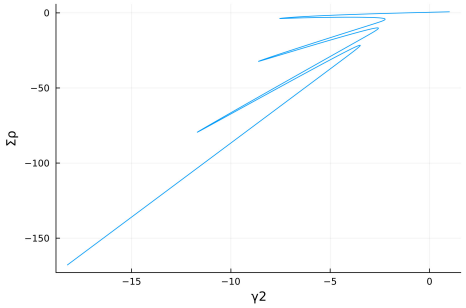

Figure 20: Bifurcation diagram for the modified Bastiaansen system using a grid stretched by a factor of -1.

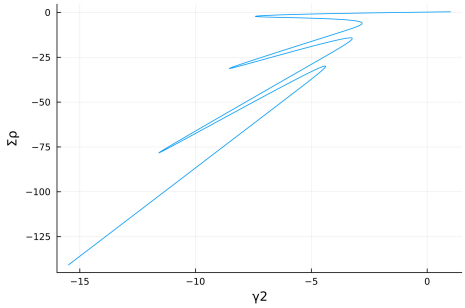

Figure 21: Bifurcation diagram for the modified Bastiaansen system using a grid stretched by a factor of -10.

Finally, using $i_{\Delta}^{res} = 0.1$ and $(nx, nz) = (10, 6)$ on an unstretched grid, we turn on the diffusion in the vertical direction. Figures 22 and 23 show the appearance of new bifurcations, as expected from the analytical eigenvalue analysis.

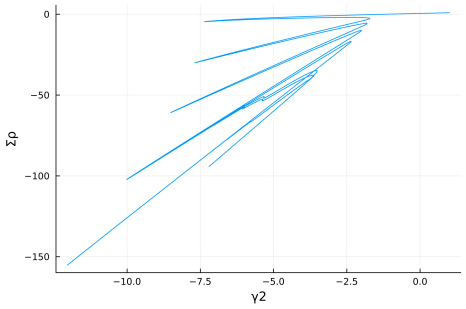

Figure 22: Bifurcation diagram for the modified Bastiaansen with diffusion turned on in the vertical direction.

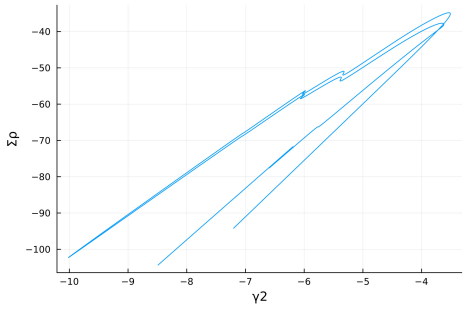

Figure 23: Detail of the new bifurcations (the rest of the bifurcation diagram is not plotted).

4.4 Discussion

Firstly we would like to attempt to explain the dependancy of the number of folds on the number of grid points. To that aim, note that a change of coordinates

$$\rho \mapsto 10\rho + \frac{z}{2}$$

transforms the convective adjustment function of this system back into the convective adjustment function used in the decoupled den Toom system. For this (one-dimensional) system a discrete version of the weak formulation was derived [15], this is

$$\frac{n_z^2}{P_v} \sum_{k=1}^{nz-1} ([1 + \overline{C} + n_z \overline{C'} \cdot (\overline{\rho}_{k+1} - \overline{\rho_k})][\Delta\rho_{k+1} - \Delta\rho_k]^2) = (-i_+^{res} + \lambda) \sum_{k=1}^{n_z} |\Delta\rho_k|^2.$$

From this equation it was argued that the diffusion feedback may operate at the level of the interfaces and that the value of $\overline{C}$ would strongly depend on the resolution. In our case the same mechanism is likely at play, however given the grid dependency is in the horizontal direction, it would seem less likely that the resolution-dependency of $\overline{C}$ is what is causing the multiple folds, as seen in figure 26 it is much more plausible that these are due to the diffusion feedback acting at the interface level.

We have thus seen that a system which in one-dimension exhibits no spurious multiple equilibria can in fact present what may be spurious equilibria when considered in two spatial dimensions. This would suggest that in fact the analytical system may have some bifurcations, which could then fragment as discussed in section 2.

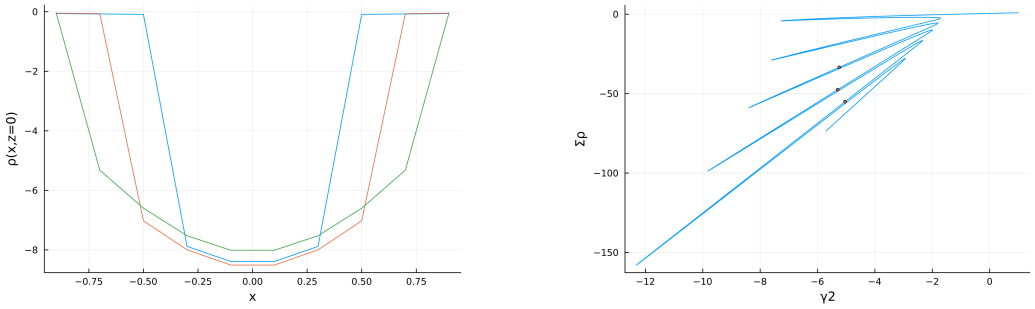

Figure 24: Three solution profiles at $z = 0$ (left) corresponding to the equilibria dotted in red in the bifurcation diagram (right).

5 Spuriousness of the multiple equilibria in the original den Toom models

The bifurcation structure we have seen so far is referred to in the literature as *snaking*. The most typical form of these is due to a homoclinic orbit (see e.g. [7, 9]) forming in the spatial dynamics of the system, however sometimes this has to do with Turing bifurcations destabilising travelling fronts [2] or with localised Turing patterns that grow increasingly larger in the spatial domain [12]. We thus check the den Toom systems in their original formulation for the possibility of homoclinic orbits in the spatial dynamics and Turing instabilities.

5.1 Spatial Dynamics of the den Toom model

Note that, dropping horizontal diffusion from system (1), we can rewrite its steady state equation as

$$\begin{aligned}
\frac{\partial^2 \rho}{\partial z^2} &= \frac{i_+^{res}\rho + i_-^{res}\mu - \overline{\rho}}{1 + \frac{\partial \rho}{\partial z}C'(\frac{\partial \rho}{\partial z}) + C(\frac{\partial \rho}{\partial z})} P_v \\
\frac{\partial^2 \mu}{\partial z^2} &= -\frac{\frac{\partial \mu}{\partial z}\frac{\partial^2 \rho}{\partial z^2}C'(\frac{\partial \rho}{\partial z})}{1 + C(\frac{\partial \rho}{\partial z})} + \frac{i_-^{res}\rho + i_+^{res}\mu - \overline{\mu}}{1 + C(\frac{\partial \rho}{\partial z})} P_v.
\end{aligned}$$

Now let $x_1 = \rho$ and $x_2 = \mu$, the above system can then be written as

$$\begin{aligned}
\dot{x}_1 &= y_1 \\
\dot{y}_1 &= \frac{i_+^{res}x_1 + i_-^{res}x_2 - \gamma\cos(\pi z) + \cos(2\pi z)}{1 + y_1 C'(y_1) + C(y_1)} P_v \\
\dot{x}_2 &= y_2 \\
\dot{y}_2 &= -\frac{y_2 \dot{y}_1 C'(y_1)}{1 + C(y_1)} + \frac{i_-^{res}x_1 + i_+^{res}x_2 - \gamma\cos(\pi z) - \cos(2\pi z)}{1 + C(y_1)} P_v.
\end{aligned}$$

This system is non-autonomous, however it is equivalent to the autonomous system given by

$$\dot{x}_1 = y_1 \tag{6a}$$

$$\dot{y}_1 = \frac{i_+^{res} x_1 + i_-^{res} x_2 - \gamma\cos(\pi z) + \cos(2\pi z)}{1 + y_1 C'(y_1) + C(y_1)} P_v \tag{6b}$$

$$\dot{x}_2 = y_2 \tag{6c}$$

$$\dot{y}_2 = -\frac{y_2 \dot{y}_1 C'(y_1)}{1 + C(y_1)} + \frac{i_-^{res} x_1 + i_+^{res} x_2 - \gamma\cos(\pi z) - \cos(2\pi z)}{1 + C(y_1)} P_v \tag{6d}$$

$$\dot{z} = 1. \tag{6e}$$

5.1.1 Decoupled case

Choosing $i_+^{res} = 1$ and $i_-^{res} = 0$ in system (6) and discarding equations (6c) and (6d), we obtain

$$\begin{aligned}
\dot{x} &= y =: f_1(x, y, z) \\
\varepsilon\dot{y} &= \frac{x - \gamma\cos(\pi z) + \cos(2\pi z)}{1 + y\,\mathrm{sech}^2(10y) + 50(1 + \tanh(10y))} =: f_2(x, y, z) \\
\dot{z} &= 1 =: f_3(x, y, z),
\end{aligned}$$

where we are again using $\mathcal{F}_1$, we have dropped the indices for notational simplicity, and we have relabelled $\frac{1}{P_v} =: \varepsilon$ since it is possible to interpret the vertical Peclet number as a time scale parameter.

In the multiple time scales approach [8], the layer problem is found by changing the time scale to $\tau = \frac{1}{\varepsilon}t$ and taking the singular limit ($\varepsilon \to 0$). This gives

$$\begin{aligned}
\dot{x} &= 0 \\
\dot{y} &= \frac{x - \gamma\cos(\pi z) + \cos(2\pi z)}{1 + y\,\mathrm{sech}^2(10y) + 50(1 + \tanh(10y))} \\
\dot{z} &= 0.
\end{aligned}$$

from which we can obtain the critical manifold, given by

$$S = \{(x, y, z) \in \mathbb{R}^3 \quad | \quad x = \gamma\cos(\pi z) - \cos(2\pi z)\}.$$

However when one looks at the eigenvalue

$$\frac{\partial}{\partial y} f_2(x, y, z) = \frac{(20y\tanh(10y) - 501)\,\mathrm{sech}^2(10y)(x - \gamma\cos(\pi z) + \cos(2\pi z))}{(1 + y\,\mathrm{sech}^2(10y) + 50(1 + \tanh(10y)))^2}$$

it becomes clear that for $(x, y, z) \in S$, $\frac{\partial f_2}{\partial y} = 0$ and so

$$L = S.$$

That is: the subset of fold points of the critical manifold (i.e. L) is in fact the entire critical manifold. Thus the lens of multiple time scales can say nothing about the dynamics of the system.

5.1.2 Coupled case

Using $i_+^{res} = \frac{1}{2}$ and $i_-^{res} = -\frac{1}{2}$ in system (6) and again interpreting $\frac{1}{P_v} =: \varepsilon$ as a time scale parameter the layer problem is given by the system

$$\begin{aligned}
\dot{x}_1 &= 0 \\
\dot{y}_1 &= \frac{\frac{1}{2}x_1 - \frac{1}{2}x_2 - \gamma\cos(\pi z) + \cos(2\pi z)}{1 + y_1 C'(y_1) + C(y_1)} \\
\dot{x}_2 &= 0 \\
\dot{y}_2 &= -\frac{y_2 \dot{y}_1 C'(y_1)}{1 + C(y_1)} + \frac{-\frac{1}{2}x_1 + \frac{1}{2}x_2 - \gamma\cos(\pi z) - \cos(2\pi z)}{1 + C(y_1)} \\
\dot{z} &= 0.
\end{aligned}$$

which has for equilibria

$$(x_1, x_2, y_1, y_2, z) = (x_1, x_1 - 2\cos((n + \frac{1}{2})2\pi), y_1, y_2, n + \frac{1}{2}), \quad n \in \mathbb{Z}.$$

We henceforth consider $z \in \mathbb{R}/2\mathbb{Z}$ for simplicity. The critical manifolds are then

$$\begin{aligned}
S_1 &= \{(x_1, x_2, y_1, y_2, z) \in \mathbb{R}^4 \times \mathbb{R}/2\mathbb{Z} \quad | \quad x_1 = x_2 - 2, \text{ and } z = \frac{1}{2}\} \\
S_2 &= \{(x_1, x_2, y_1, y_2, z) \in \mathbb{R}^4 \times \mathbb{R}/2\mathbb{Z} \quad | \quad x_1 = x_2 + 2, \text{ and } z = \frac{3}{2}\}.
\end{aligned}$$

Next we have that

$$\begin{aligned}
\frac{\partial f_2}{\partial y_1} =& -\frac{y_1 C''(y_1) + 2C'(y_1)}{1 + y_1 C'(y_1) + C(y_1)} f_2 \\
\frac{\partial f_2}{\partial y_2} =& 0 \\
\frac{\partial f_4}{\partial y_1} =& -y_2 \frac{(C'(y_1)^2 - (C(y_1) + 1)C''(y_1))f_2 - (C(y_1) + 1)C'(y_1)\frac{\partial f_2}{\partial y_1}}{C(y_1) + 1} \\
& - \frac{\frac{1}{2}(x_2 - x_1) - (\gamma\cos(\pi z) + \cos(2\pi z)}{1 + C(y_1)} C'(y_1) \\
\frac{\partial f_4}{\partial y_2} =& -\frac{C'(y_1)}{1 + C(y_1)} f_2,
\end{aligned}$$

note that for $(x_1, x_2, y_1, y_2, z) \in S_i$ we have that

$$\frac{\partial f_2}{\partial y_1} = \frac{\partial f_2}{\partial y_2} = \frac{\partial f_4}{\partial y_1} = \frac{\partial f_4}{\partial y_2} = 0$$

and thus again

$$L_1 = S_1, \quad L_2 = S_2.$$

So the analysis using geometric singular perturbation theory is invalid also in the coupled case.

5.2 Localized Turing Instability

Consider a reaction diffusion system of the form

$$\frac{\partial U}{\partial t} = D_U \nabla^2 U + f(U,V)$$
$$\frac{\partial V}{\partial t} = D_V \nabla^2 V + g(U,V)$$

(where f and g are nonlinear). Suppose that $(\overline{U}, \overline{V})$ is an equilibrium, the linearization of the above system around this equilibrium is then

$$\frac{\partial \Delta U}{\partial t} = D_U \nabla^2 \Delta U + f_U(\overline{U},\overline{V})\Delta U + f_V(\overline{U},\overline{V})\Delta V$$
$$\frac{\partial \Delta V}{\partial t} = D_V \nabla^2 \Delta V + g_U(\overline{U},\overline{V})\Delta U + g_V(\overline{U},\overline{V})\Delta V.$$

To this system, we guess a solution of the form $(\Delta U, \Delta V) = e^{\lambda t + ikx}$. Substituting this in the above, we may obtain a *dispersion relation* of the form

$$\lambda = h(k).$$

It then follows that the eigenvalue λ may be of different sign for different wavenumbers k, implying that it is possible that only some eigenmodes (i.e. solutions to the linearized system) may bifurcate. This situation defines a *Turing bifurcation* [14], which is often responsible for pattern formation in the solutions of the original reaction-diffusion model.

In this section we explore the possibility of the presence of a *localized* Turing bifurcation in the coupled den Toom system. This kind of situation can occur in reaction diffusion systems with spatially varying coefficients, where some eigenmodes lose stability only within a finite region of the spatial domain. This typically results in localized patterns within that region. To this aim, let us define

$$J(z) = \begin{bmatrix} -i_+^{res} & -i_-^{res} \\ -i_-^{res} & -i_+^{res} \end{bmatrix}$$
$$D(z) = \begin{bmatrix} 1 + \overline{C} + \overline{C}' \frac{\partial \overline{\rho}}{\partial z} & 0 \\ \overline{C}' \frac{\partial \overline{\mu}}{\partial z} & 1 + \overline{C} \end{bmatrix}$$
$$M(z) = \begin{bmatrix} (\frac{\partial \overline{\rho}}{\partial z} + \frac{\partial \overline{\rho}^2}{\partial z^2})\overline{C}' + (\frac{\partial \overline{\rho}}{\partial z})^2 \overline{C}'' & 0 \\ \frac{\partial^2 \overline{\mu}}{\partial z^2}\overline{C}' + \overline{C}\frac{\partial \overline{\mu}}{\partial z}\frac{\partial \overline{\rho}}{\partial z} & \overline{C}' \frac{\partial \overline{\rho}}{\partial z} \end{bmatrix}$$
$$N(z) = 0$$

we may then write $(\Delta\rho, \Delta\mu) =: w$, $\frac{1}{P_v} =: \varepsilon^2$ and the linearized system (3) as

$$\frac{\partial w}{\partial t} = \varepsilon^2 (D(z)\frac{\partial^2 w}{\partial z^2} + M(z)\frac{\partial w}{\partial z} + N(z)w) + J(z)w. \tag{7}$$

Further define $B_0(z) = D(z)^{-1}J(z)$. Throughout this section we will use the following theorem [5]:

Theorem 5.1. *Let $0 < \varepsilon \ll 1$ and assume that $\mathrm{tr}(B_0(x))^2 - 4\det(B_0(x))$ has only simple zeros for all $x \in [0,1]$. Further, assume stability to homogeneous perturbations, i.e.*

$$\mathrm{tr}(J(x)) < 0, \quad \det(J(x)) > 0 \quad \forall x \in [0,1]$$

Then, subject to a wave selection constraint, which can always be satisfied by sufficiently small diffusion scale, there exists a non-homogeneous, bounded and nontrivial solution w to equation (7) and homogeneous Neumann boundary conditions at $x \in \{0,1\}$ that grows exponentially in time only within the interval $\mathcal{T}_0$ if

$$\mathrm{tr}(B_0(x)) > 0, \quad [\mathrm{tr}(B_0(x))]^2 - 4\det(B_0(x)) > 0, \quad \textit{for all } x \in \mathcal{T}_0, \tag{8}$$

where $\mathcal{T}_0$ is the largest subset of $[0,1]$ where conditions (8) hold.

Note that Turing bifurcations have sofar only been observed in systems of 2 equations, thus we can only check the coupled den Toom system. In this case $\det(J(x)) = 0$, since we picked $i_+^{res} = -i_-^{res} = \frac{1}{2}$, however for the sake of argument we will pick

$$i_+^{res} = \frac{1}{2} + \alpha$$
$$i_-^{res} = -\frac{1}{2} + \alpha$$

for $\alpha \ll 1$. In this case we have

$$\det(J(x)) = (\frac{1}{2} + \alpha)^2 - (-\frac{1}{2} + \alpha)^2 = 2\alpha > 0.$$

Figure 27 shows a bifurcation diagram for the aforementioned choice of i_+^{res} and i_-^{res}, we see that this is in fact qualitatively equivalent to the bifurcation diagram in section 2.4.1. Finally, note that

$$\cos(\pi z) = \cos(-\pi z), \quad \cos(2\pi z) = \cos(-2\pi z)$$

so in principle we could switch the domain to $z \in [0,1]$ and obtain the same results. Now we have that

$$B_0(z) = D(z)^{-1}J(z) = \begin{bmatrix} \frac{1}{1+\overline{C}+\overline{C}'\frac{\partial\overline{\rho}}{\partial z}} & 0 \\ -\frac{\overline{C}'\frac{\partial\overline{\mu}}{\partial z}}{(1+\overline{C}+\overline{C}'\frac{\partial\overline{\rho}}{\partial z})(1+\overline{C})} & \frac{1}{1+\overline{C}} \end{bmatrix} \begin{bmatrix} -i_+^{res} & -i_-^{res} \\ -i_-^{res} & -i_+^{res} \end{bmatrix}$$
$$= \begin{bmatrix} -\frac{i_+^{res}}{1+\overline{C}+\overline{C}'\frac{\partial\overline{\rho}}{\partial z}} & -\frac{i_-^{res}}{1+\overline{C}+\overline{C}'\frac{\partial\overline{\rho}}{\partial z}} \\ \frac{i_+^{res}\overline{C}'\frac{\partial\overline{\mu}}{\partial z} - i_-^{res}(1+\overline{C}+\overline{C}'\frac{\partial\overline{\rho}}{\partial z})}{(1+\overline{C}+\overline{C}'\frac{\partial\overline{\rho}}{\partial z})(1+\overline{C})} & \frac{i_-^{res}\overline{C}'\frac{\partial\overline{\mu}}{\partial z} - i_+^{res}(1+\overline{C}+\overline{C}'\frac{\partial\overline{\rho}}{\partial z})}{(1+\overline{C}+\overline{C}'\frac{\partial\overline{\rho}}{\partial z})(1+\overline{C})} \end{bmatrix}$$

so that

$$\det(B_0(z)) = \frac{((i_-^{res})^2 - (i_+^{res})^2)}{(1+\overline{C})(1+\overline{C}+\overline{C}'\frac{\partial\rho}{\partial z})}$$
$$\mathrm{tr}(B_0(z)) = \frac{i_-^{res}\overline{C}'\frac{\partial\mu}{\partial z} - i_+^{res}(2+2\overline{C}+\overline{C}'\frac{\partial\overline{\rho}}{\partial z})}{(1+\overline{C})(1+\overline{C}+\overline{C}'\frac{\partial\rho}{\partial z})}.$$

Figure 25 shows the points at which condition (8) is verified for the perturbed system, when using C_n to numerically approximate the condition.

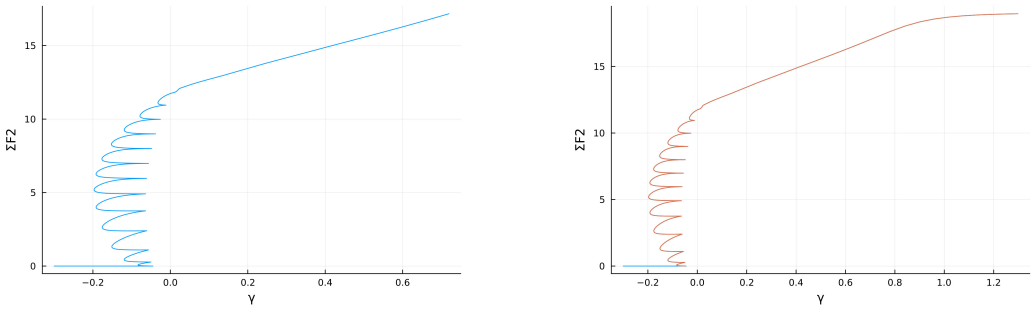

Figure 25: Bifurcation diagram for the perturbed coupled den Toom system with $n_z = 20$ and $\alpha = 10^{-3}$ (left). Points at which condition (8) is verified when using C_n (right, red).

Note that for $\gamma > 1$ the localized instability is considerably small and thus the condition is likely only verified due to numerical accuracy. The same holds on the lower side of the fold bifurcations. The localized instability seems to only really occur at a point. This explains the absence of visible patterns in the solutions. This pointwise instability travels (as γ is varied) at each successive fold a distance $\frac{1}{nz}$ from $z = -1$ to $z = 0$, and regains stability along the stable branches of the fold bifurcations. The localized Turing instability would however seem to overlap with the area in the bifurcation diagram where the system (in absence of horizontal diffusion) has a persistent Hopf bifurcation, this could suggest that the snaking is due to the destabilisation of a yet undetected travelling wave (see e.g. [3, 6]). The structure of the snaking however is particular: the equilibrium leaves the snaking region in the opposite direction from where it came, this has been observed near codimension 3 bifurcations [13] and is dubbed *twisted snaking*.

6 Conclusion

In section 3, we have shown that if there are any non-spurious bifurcations in the den Toom models, these may exhibit fragmented tipping if more than one spatial dimension (with relative heterogeneity and diffusion) is accounted for. Next, in section 4 we observed how a related system which in one dimension does not exhibit spurious bifurcations, in two dimensions exhibits a very similar bifurcation structure to that of the den Toom models, which following the arguments made in [15] would also seem to be spurious. It is worth noting at this stage that an analytical solution was found in [15] when using the Heaviside step function as convective adjustment, so in principle fragmented tipping could be causing some of the multiple equilibria observed in [11]. In section 5.1 have also attempted to check if there is any bifurcations in the spatial dynamics, as these may cause the snaking we observe, however this route proves to be inconclusive as it requires insight from the theory of non autonomous dynamical systems. Finally in section 5.2 we found what would appear to be a localised (pointwise) Turing bifurcation, which further study may show is responsible for the occurrence of the snaking.

From an Oceanographic standpoint however, it still holds that the multiple equilibria are due to the convective adjustment. This is an artificial implementation in large scale ocean circulation models to prevent an unstable stratification from occurring. Perhaps a better representative conceptual model to study the physics underlying the effects of increased freshwater forcing on the AMOC would come from modifying a differentially heated lid-driven cavity [4] to include salinity and freshwater forcing.

References

[1] Bastiaansen, R., Dijkstra, H.A., von der Heydt, A.S., 2022. Fragmented tipping in a spatially heterogeneous world. Environ. Res. Lett. 17 045006.

[2] Carter, Paul, et al. "Criteria for the (in) stability of planar interfaces in singularly perturbed 2-component reaction–diffusion equations." Physica D: Nonlinear Phenomena 444 (2023): 133596.

[3] Champneys AR, Al Saadi F, Breña–Medina VF, Grieneisen VA, Marée AFM, Verschueren N, Wuyts B, Bistability, wave pinning and localisation in natural reaction–diffusion systems, Physica D: Nonlinear Phenomena, Volume 416, 2021

[4] Dijkstra HA, Wubs FW. Bifurcation Analysis of Fluid Flows. Cambridge University Press; 2023

[5] Gaffney, E.A., Krause, A.L., Maini, P.K., Wang, C. Spatial heterogeneity localizes Turing patterns in reaction-cross-diffusion systems. Discrete and Continuous Dynamical Systems - B, 2023, 28(12): 6092-6125.

[6] Ghazaryan, Anna, and Björn Sandstede. "Nonlinear convective instability of Turing-unstable fronts near onset: a case study." SIAM Journal on Applied Dynamical Systems 6.2 (2007): 319-347.

[7] Houghton, S. M., and E. Knobloch. "Homoclinic snaking in bounded domains." Physical Review E—Statistical, Nonlinear, and Soft Matter Physics 80.2 (2009): 026210.

[8] Kuehn C. Multiple Time Scale Dynamics. Springer; 2015

[9] Kusdiantara, R., Susanto, H. (2017). Homoclinic snaking in the discrete Swift-Hohenberg equation. Physical Review E, 96(6), 062214.

[10] Kuznetsov YA. Elements of Applied Bifurcation Theory. Springer; 2023

[11] Lohmann, J., Dijkstra, H.A., Jochum, M., Lucarini, V., Ditlevsen, P.D., 2024. Multistability and intermediate tipping of the Atlantic Ocean circulation.Sci. Adv.10,eadi4253(2024).

[12] McCullen, Nick, and Thomas Wagenknecht. "Pattern formation on networks: from localised activity to Turing patterns." Scientific reports 6.1 (2016): 27397.

[13] Parra-Rivas, Pedro, et al. "Organization of spatially localized structures near a codimension-three cusp-Turing bifurcation." SIAM Journal on Applied Dynamical Systems 22.4 (2023): 2693-2731.

[14] Song, W. (2019). Matrix-based techniques for (flow-)transition studies. [Thesis fully internal (DIV), University of Groningen]. University of Groningen.

[15] den Toom, M., Dijkstra, H.A., Wubs, F.W., 2011. Spurious multiple equilibria induced by convective adjustment. Ocean Modelling 38. 126-127.

[16] Wang, Xiaofeng & Li, Yang. (2017). An Efficient Sixth-Order Newton-Type Method for Solving Nonlinear Systems. Algorithms. 10. 45. 10.3390/a10020045.

[17] Welander, P. 1982 A simple heat-salt oscillator. Dyn. Atmos. Oceans 6. 233-42